NEMESIS
Negative Effects in Medical Sciences Oral and Maxillofacial Surgery
UCL PRESSES UNIVERSITAIRES DE LOUVAIN

Supernumerary teeth in premolar and molar area on CBCT: a pictorial review.

Authors:
Olszewski R DDS,MD,PhD,DrSc,Prof[1,2,ϕ*],
Shimwa-Karengera S[1,ϕ] MD,DDS,
Gurniak A[3] DDS,
Gurniak E[3] DDS,
Serve A[4], BDS,
Simain Sato F[5] DDS,PhD

Affiliations:

[1] Department of oral and maxillofacial surgery, Cliniques universitaires saint Luc, UCLouvain, Av. Hippocrate 10, 1200 Brussels, Belgium
[2] Oral and maxillofacial surgery research lab (OMFS Lab), NMSK, Institut de recherche expérimentale et Clinique (IREC), SSS, UCLouvain, Brussels, Belgium
[3] Diagdent, ul. Brazylijska 13, Warszawa, Poland
[4] Ecole de médicine dentaire et stomatologie, UCLouvain, Av. Hippocrate 10, 1200, Brussels, Belgium
[5] Université de Liège, 7 Place du 20 Août, 4000, Liège, Belgium
[ϕ] First equivalent authors

Corresponding author: Prof R. Olszewski, Olszewski, Department of Oral and maxillofacial surgery, Cliniques universitaires saint Luc, UCLouvain, Brussels, Begium; phone+3227645718; fax: +3227645876; OCIDiD:orcid.org/0000-0002-2211-7731

Disclaimer: the views expressed in the submitted article are our own and not an official position of the institution or funder.

Abstract

Objective: to build a descriptive classification of premolar and molar supernumerary teeth (ST) when preparing the cone beam computed tomography (CBCT) report. The aim is also to share wide range of CBCT images in the open access publishing model.

Material and methods: For our review we systematically searched for articles from PubMed with 1) free full texts on ST in molar and premolar area and using CBCT, and 2) articles providing with information on complications related with the presence of ST in molar and premolar area. We also added to our review studies providing with classic ST classifications in premolar and molar area.

Results: We found 29 cases of ST, and we freely illustrated them with 84 figures. We separated our pictorial review in: 1) unilateral ST in the mandible, 2) unilateral ST in the maxilla, 3) unilateral undersized ST, 4) bilateral ST, 5) ST with additional features, and 6) cases with major hyperdontia.

Conclusions: we build up the classification matrix for premolar and molar ST with 11 descriptors and 50 boxes. The descriptors were: 1) location if the ST crown in axial view, 2) vertical location of the cusp tip in relation with closest erupted tooth in coronal view, 3) shape, 4) distribution, 5) Position (in relation to normal tooth eruption) in sagittal view, 6) State of eruption of the ST in the sagittal view, 7) Follicle size measurement in sagittal view, 8) External root resorption of adjacent teeth by ST and its location in relation to the long axis of the involved tooth, 9) Internal resorption of ST, 10) Adjacent tooth complication, and 11) Damage to surrounding structures if ST removal. The open access figures from the literature illustrated 11 boxes. With our pictorial review we were able to illustrate 45 out of 50 boxes, and freely provide the readership with the most complete description of ST in premolar and molar area on CBCT than in previously published studies.

Keywords: supernumerary teeth, CBCT, premolar, molar, cone beam computed tomography

Introduction

Supernumerary teeth (ST) are additional teeth to decidual or permanent dentition [1] Their prevalence varies among diverse human populations, and ranges between 0.1 to 4% [1]. They can be found as incidental finding or as the explanation of trouble of teeth eruption on panoramic radiography. However panoramic radiography is related with deformations, and superimpositions and may be of limited value for ST diagnostic [1]. It is currently replaced by cone beam computed tomography (CBCT) [2] especially for the diagnostic of ST in orthodontics [3-5]. Eleven types of classifications of ST were already proposed in the literature [6-17]. The ST were all classified in relation to the morphology/shape, and location [7-17]. Seven classifications of ST were based on conventional dental radiography used before the era of CBCT [7-13]. Four classifications were only related with the description of anterior ST [7-9, 13]. Seven articles presented with specific classifications for ST in premolar and molar area [10-12, 14-17]. Complications related to ST were present only in one classification [16]. All articles published after 2003, and related to the ST classifications provided with no CBCT reference figures [14-17]. Only one article from 1999 [12] was accessible in open access but without any CBCT reference figure.

The aim of our study was to build a descriptive classification matrix to allow for the most complete description of premolar and molar ST when writing the CBCT report. We wanted to compile already known classifications with information from studies on complications related with ST, and depicted on CBCT. We wanted also to provide the readership with illustrations of diverse types and situations related with premolar and molar ST from available references figures found in open access literature, and from our University Clinic CBCT collection. We wanted share the images in the open access publishing model; allowing anyone to use these images, parts of the text or a full article (under the condition of correctly citing the source and sharing in the open access as well CC BY SA).

Materials and methods

For our review we searched first for articles with free full texts on ST in molar and premolar area and using CBCT. We used only one database-PubMed. There was no limit of time for the search. We selected only English language articles. The search equation was set as follow: ((("tooth, supernumerary"[MeSH Terms] OR ("tooth"[All Fields] AND "supernumerary"[All Fields]) OR "supernumerary tooth"[All Fields] OR ("supernumerary"[All Fields] AND "teeth"[All Fields]) OR "supernumerary teeth"[All Fields]) AND "CBCT"[All Fields]) AND (ffrft[Filter]). The search was performed on 13.11.2021. One observer performed the search. The inclusion criteria were: ST present in molar and premolar area (from mesial to first premolar to mesial to third molar), and presence of figures from CBCT depicting morphology and

location of ST. The exclusion criteria were ST found between canines, patients with syndromes, animal studies, experimental studies, and articles without access to free pdf format even if taged as a free full text. We found 45 articles, with 41 articles excluded and 4 articles included in this review [2, 18-20].

Moreover, we searched for articles describing ST in molar and premolar area with the use of CBCT, and providing with information on complications related with the presence of ST. We used only one database-PubMed. There was no limit of time for the search. We selected only English language articles. The search equation was set as follow: (("tooth, supernumerary"[MeSH Terms] OR ("tooth"[All Fields] AND "supernumerary"[All Fields]) OR "supernumerary tooth"[All Fields] OR ("supernumerary"[All Fields] AND "teeth"[All Fields]) OR "supernumerary teeth"[All Fields]) AND ("complicances"[All Fields] OR "complicate"[All Fields] OR "complicated"[All Fields] OR "complicates"[All Fields] OR "complicating"[All Fields] OR "complication"[All Fields] OR "complication s"[All Fields] OR " complications"[MeSH Subheading] OR "complications"[All Fields]) AND ("retinal cone photoreceptor cells"[MeSH Terms] OR ("retinal"[All Fields] AND "cone"[All Fields] AND "photoreceptor"[All Fields] AND "cells"[All Fields]) OR "retinal cone photoreceptor cells"[All Fields] OR "cone"[All Fields]) AND "beam"[All Fields]) AND ((fha[Filter]) AND (humans[Filter]) AND (english[Filter])). The search was performed on 01.10.2021. One observer performed the search.

The inclusion criteria were articles about ST present in molar and premolar area (from mesial to first premolar to mesial to third molar) using CBCT, and describing complications related to the presence and management of ST. The exclusion criteria were ST other than molar and premolars (mesiodens, canines, incisors), and patients with syndromes.

We found 20 articles, and 6 articles were selected for the review [1, 21-25] with one open-access [21] and 5 closed access articles [1, 22-25].

Finally, we selected 17 articles for this review: 10 articles found though the PubMed search equation [1,2, 18-25], and 7 articles related to the ST classifications [10-12, 14-17].

Results

Among dentomaxillofacial CBCT reports from our University Clinics, we found 168 reports with “supernumerary” term, with 25 CBCT reports specifically related to ST in premolar and molar area. We obtained 4 additional clinical cases from colleagues from private practice using the previously described methodology using social media (Nemesis Facebook group) [26].

1. Unilateral supernumerary teeth in the mandible

Fig. 1. Patient n°1. Planmeca 3D Mid CBCT. A. Axial view. ST (*) in lingual position, between the roots of teeth n°44 and 45. B. Coronal view. Arrow: ST is erupted, of supplemental shape, and positioned at the level of the cusp of the tooth n°45.

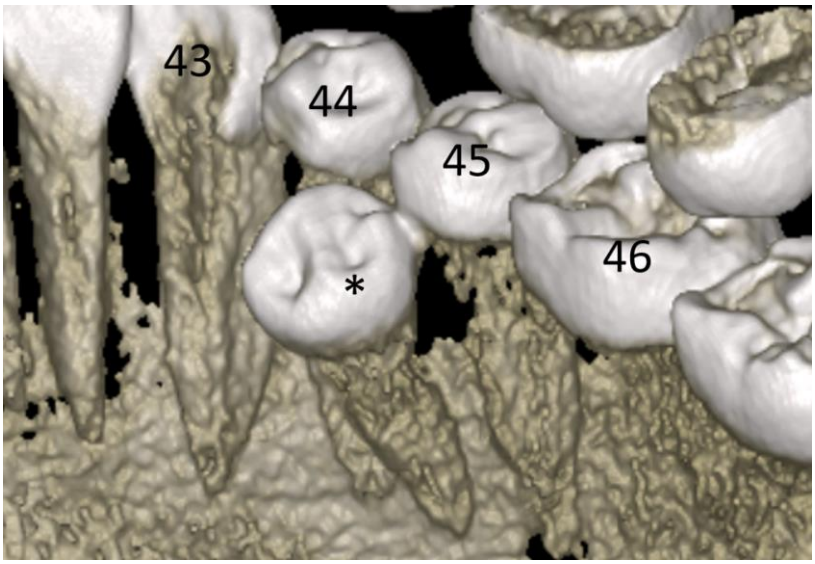

Fig. 2. Patient n°1. Planmeca 3D Mid CBCT. Lingual lateral view of the right mandible. ST (*) of supplemental shape parallel to the tooth n°45. No close relationship between the roots of ST and the roots of teeth n°44 and n°45.

Fig. 3. Patient n°2. Planmeca 3D Mid CBCT. A. Axial view. Impacted ST (*) on lingual side between the roots of teeth n°34 and n°35. Mesial rotation of tooth n°35. B. Coronal view. ST (*) is impacted, of supplemental shape, and positioned in the middle third of the adjacent roots (teeth n°34 and n°35). ST is vertical, and parallel to adjacent teeth n°34 and n°35. Thick arrow: left foramen mentale. Close relationship between the left inferior alveolar canal and the ST root.

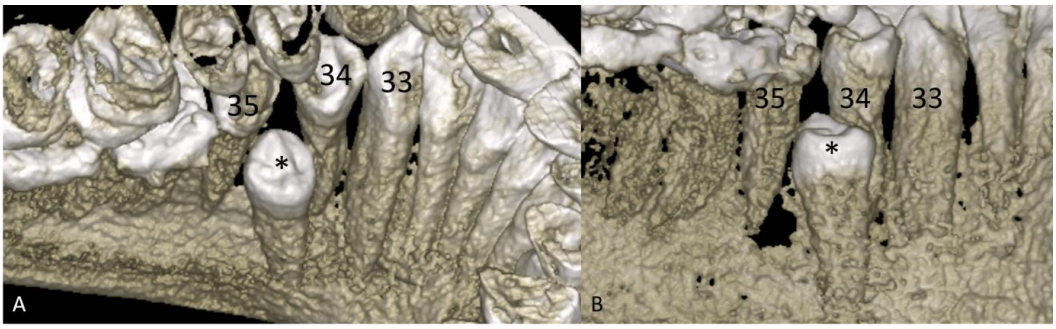

Fig. 4. Patient n°2. Planmeca 3D Mid CBCT. A. 3D occlusal and lingual view of the left mandible. Supplemental ST (*) between teeth n°34 and n°35. B. 3D lateral lingual view of the left mandible. Tooth n°35 tilted to the mesial side. ST (*) on lingual side.

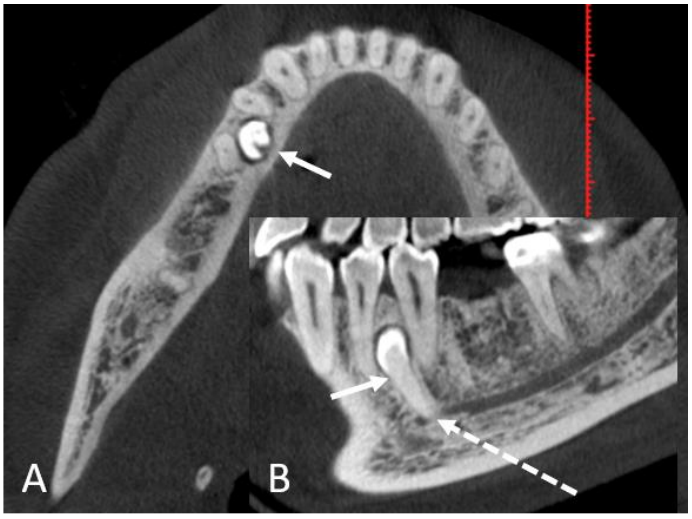

Fig. 5. Patient n°3. Planmeca 3D Mid CBCT. A. Axial view. Arrow: intra-alveolar impacted ST, between the roots of teeth n°44 and n°45. B. Para-sagittal view through the ST. Arrow: impacted ST of supplemental shape positioned in the apical third of the root of teeth n°44 and n°45. Arrow with dashes: close relationship between the root apex of ST and the right inferior alveolar nerve canal.

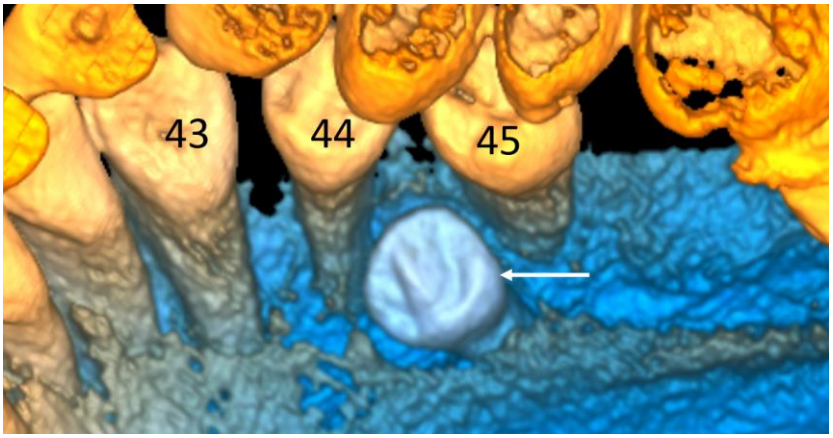

Fig. 6. Patient n°3. Planmeca 3D Mid CBCT. 3D occlusal and lingual view of the right mandible. Arrow: ST inclined to the mesial side.

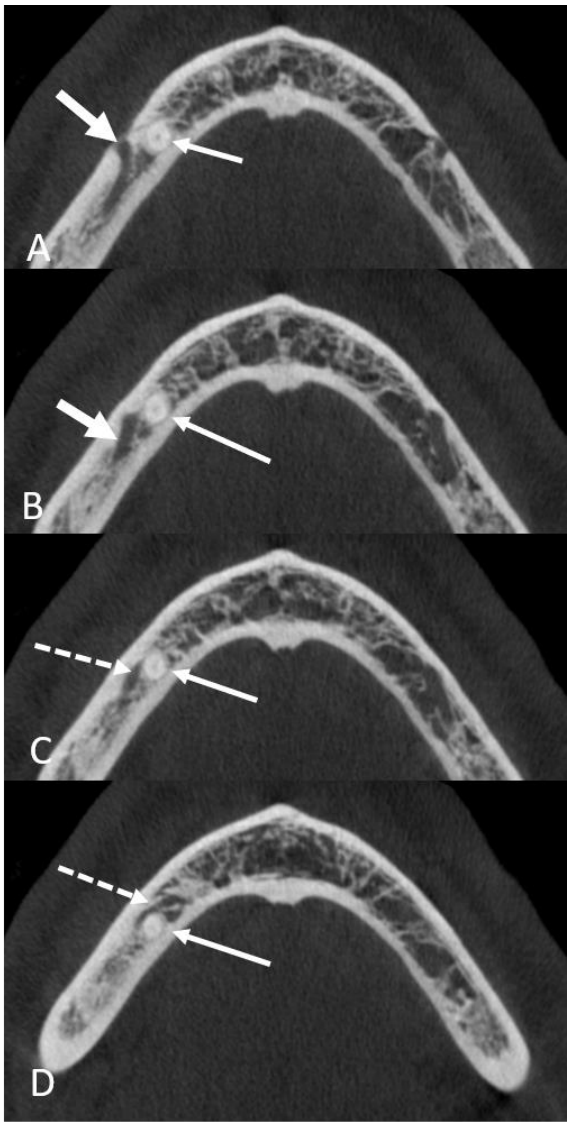

Fig. 7. Patient n°3. Planmeca 3D Mid CBCT. Axial view. A. Thick arrow: right foramen mentale. Arrow: root of ST. B. Thick arrow: right inferior alveolar nerve canal. Arrow: root of the ST. C. Additional anterior branch of right inferior alveolar nerve canal close and distal to the root of the ST (arrow). D. Additional anterior branch of the right inferior alveolar nerve canal in contact with the anterior side of the ST root (arrow).

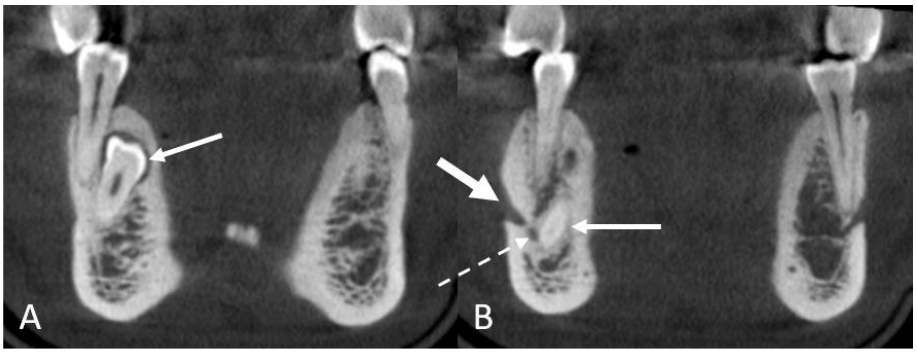

Fig. 8. Patient n°3. Planmeca 3D Mid CBCT. A. Coronal view. Arrow: impacted ST of supplemental shape on the apical third of the root of tooth n°44. B. Coronal view. Thick arrow: right foramen mentale. Arrow with dashes: Additional anterior branch of right inferior alveolar nerve canal in contact with the anterior side of the ST root (arrow).

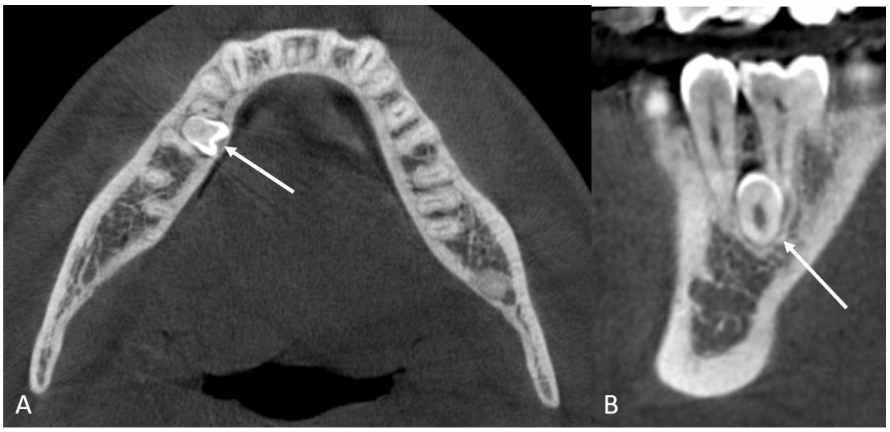

Fig. 9. Patient n°4. Planmeca 3D Mid CBCT. A. Axial view. Arrow: ST is impacted and inclined toward the lingual side. B. Sagittal view. ST (arrow) is positioned on the apical third of the roots of teeth n°45 and n°46.

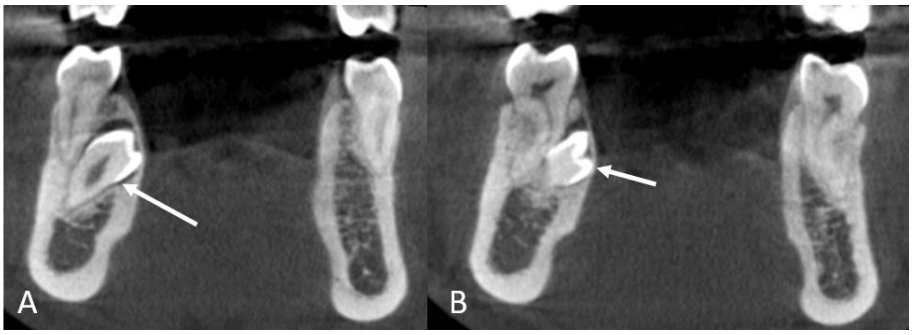

Fig. 10. Patient n°4. Planmeca 3D Mid CBCT. A. Coronal view. ST (arrow) of supplemental shape, impacted and inclined to the lingual side. Close relationship between the root of ST and the root of tooth n°45 without resorption. B. Coronal view. ST (arrow) of supplemental shape, impacted and inclined to the lingual side. Close relationship between the root of the ST and the mesial root of tooth n°46 without resorption.

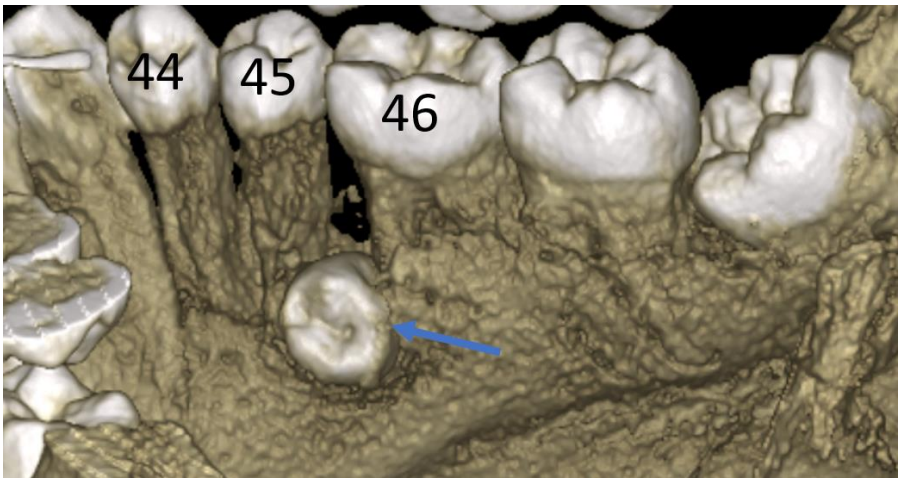

Fig. 11. Patient n°4. Planmeca 3D Mid CBCT. 3D occlusal and lingual view of the right mandible. ST (arrow) impacted, positioned on the apical third of the roots of teeth n°45 and n°46, and inclined to the lingual side.

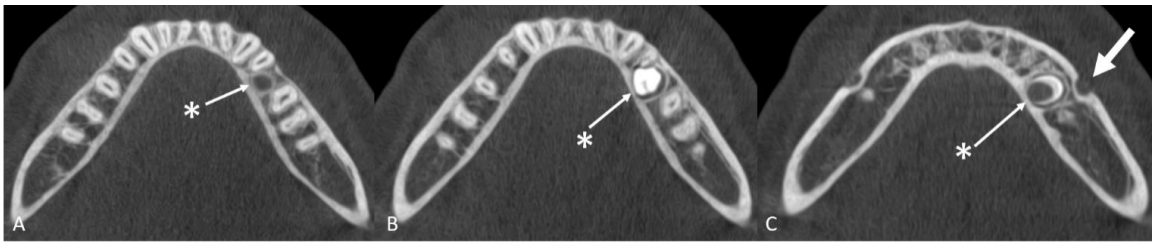

Fig. 12. Patient n°5 (15 years-old). Planmeca 3D Mid CBCT. Axial view. A. ST (*) follicle between teeth n°34 and n°35. B. ST cusp (*) in lingual position between teeth n°34 and n°35. C. ST (*) root on lingual side. Thick arrow: left foramen mentale.

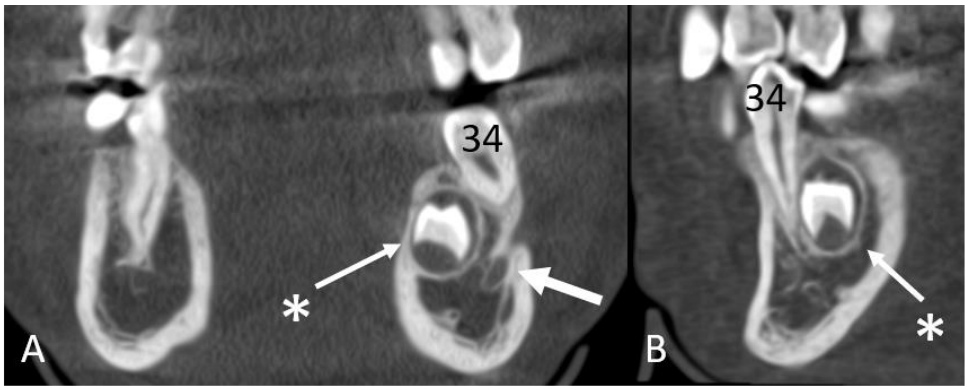

Fig. 13. Patient n°5 (15 years-old). Planmeca 3D Mid CBCT. A. Coronal view. ST (*) with the shape of a developing tooth bud. Impacted ST (*) on the lingual side at a distance from the inferior alveolar canal (thick arrow). B. Sagittal view. ST (*) is close to the apical third of the root of the tooth n°34.

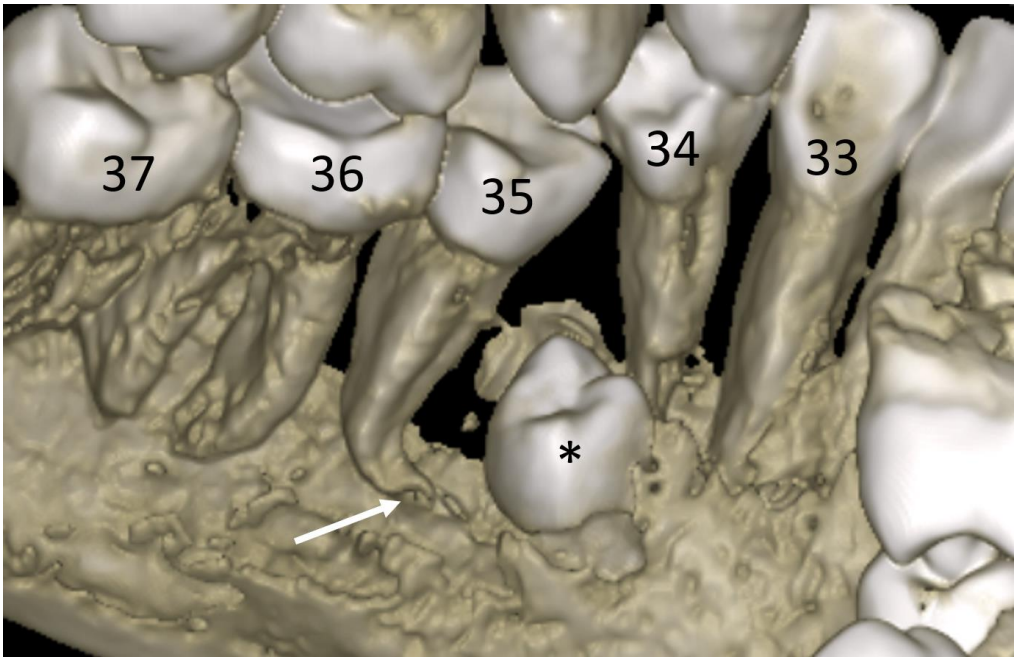

Fig. 14. Patient n°5 (15 years-old). Planmeca 3D Mid CBCT. 3D lateral lingual view of the left mandible. Tooth n°35 tilted to the mesial side. Dilaceration of the root of the tooth n°35 (arrow). ST (*) with the shape of a developing tooth bud close only to the apical third of the root of the tooth n°34.

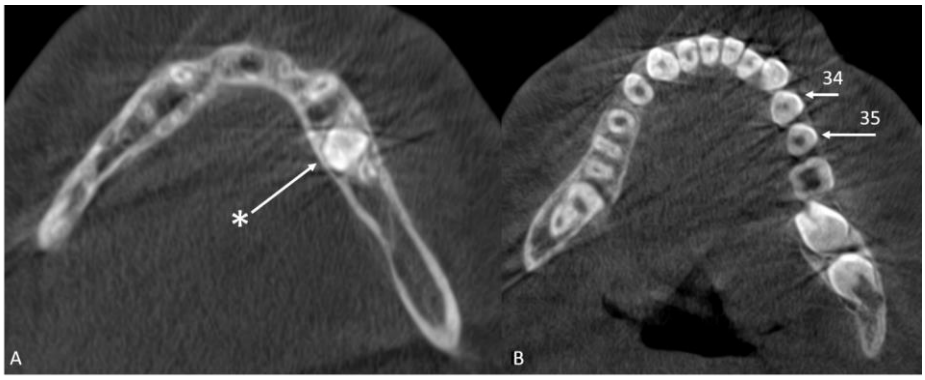

Fig. 15. Patient n°6. Planmeca 3D Mid CBCT. Axial view. A. ST (*) on the lingual side of the left mandible. B. Teeth n°34 and n°35 are rotated in the mesial direction.

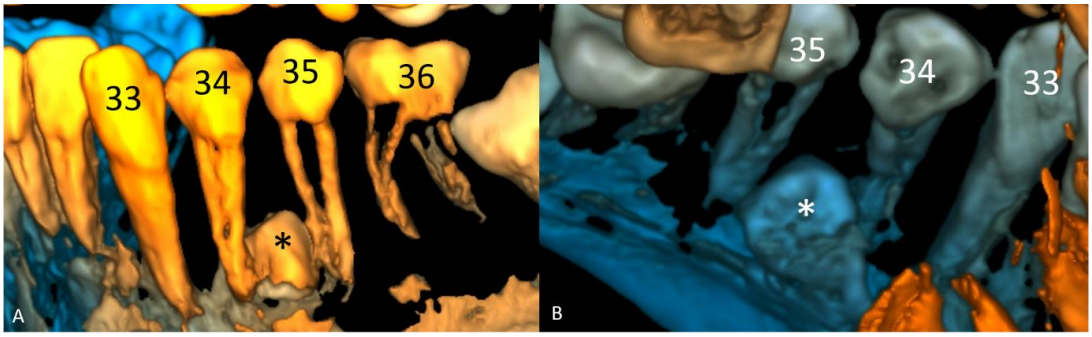

Fig. 16. Patient n°6. Planmeca 3D Mid CBCT. A. 3D lateral vestibular view of the left mandible. Impacted ST (*) with the shape of a developing tooth bud between the apical third of the root of teeth n°34 and n°35. B. 3D lateral lingual view of the left mandible. ST (*) positioned at the same distance between the roots of teeth n°34 and n°35.

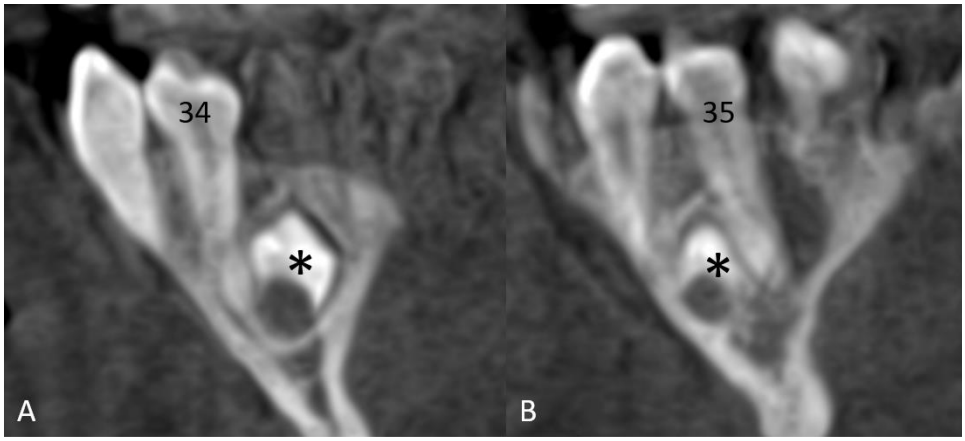

Fig. 17. Patient n°6. Planmeca 3D Mid CBCT. Sagittal view. A. ST (*) with the shape of a developing tooth bud close to the apical third of the root of the tooth n°34. B. ST (*) close to the apical third of the root of the tooth n°35.

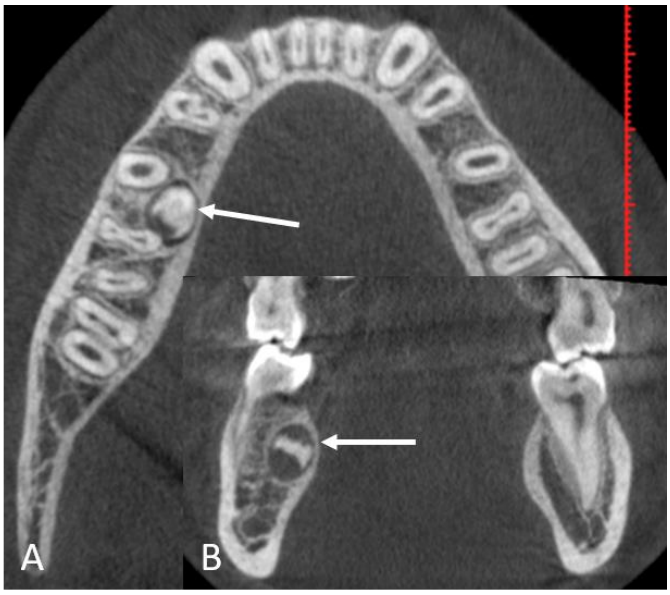

Fig. 18. Patient n°7. Planmeca 3D Mid CBCT. A. Axial view. ST (arrow) on the lingual side, between roots of teeth n°45 and n°46. B. Coronal view. ST (arrow) with the shape of a developing tooth bud impacted on the lingual side.

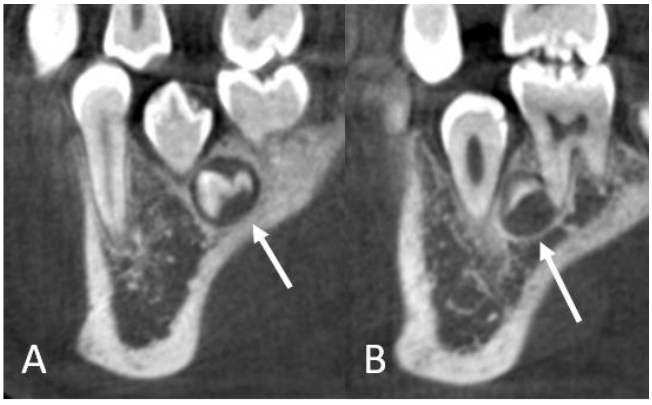

Fig. 19. Patient n°7. Planmeca 3D Mid CBCT. A. Sagittal view. ST (arrow) close to the apical third of the root of the tooth n°45. B. Sagittal view. ST (arrow) close to the apical third of the mesial root of the tooth n°46. There are no signs of external resorption of adjacent roots by ST.

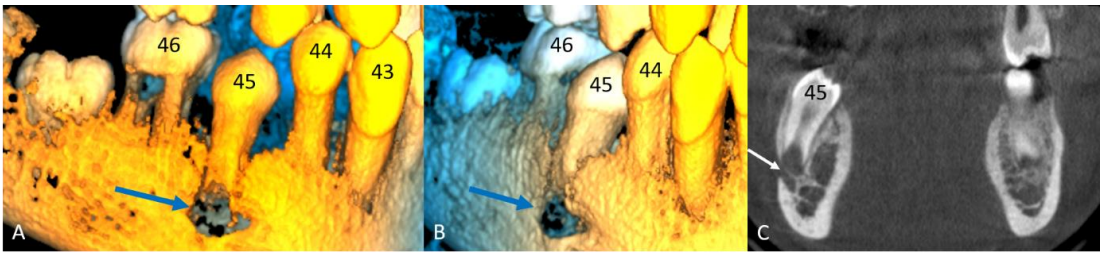

Fig. 20. Patient n°7. Planmeca 3D Mid CBCT. A. 3D lateral vestibular view of the right mandible. Tooth n°45 impacted, positioned on the vestibular side with the apex close to the right mental foramen (blue arrow). B. 3D vestibular view of the right mandible. Tooth n°45 impacted, inclined towards lingual side, and positioned on vestibular side with the apex close to the right mental foramen (blue arrow). C. Coronal view. Open apex of the tooth n°45 in close contact with the right mental foramen.

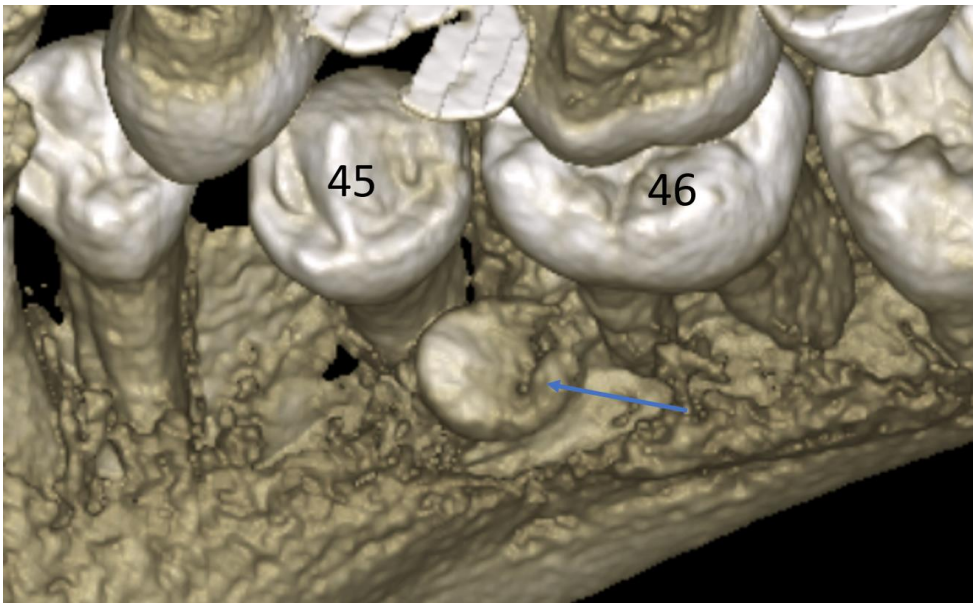

Fig. 21. Patient n°7. Planmeca 3D Mid CBCT. 3D occlusal and lingual view of the right mandible. ST (blue arrow) on the lingual side between roots of teeth n°45 and n°46.

2. Unilateral supernumerary teeth in the maxilla

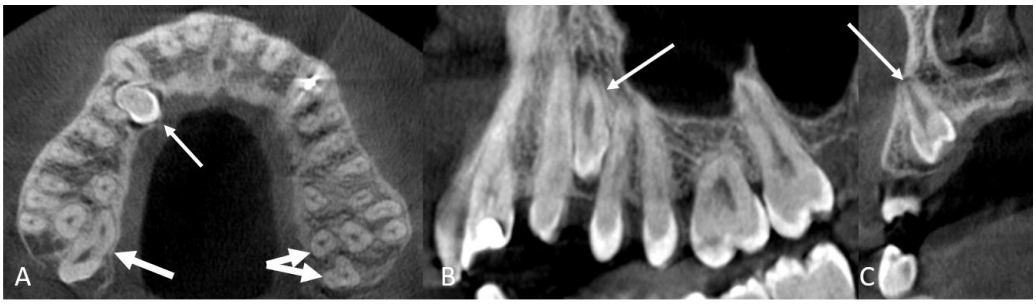

Fig. 22. Patient n°8. Planmeca 3D Mid CBCT. A. Axial view. ST (thin arrow) on palatal side between the roots of teeth n°13 and n°14. Thick arrows: dysmorphic teeth n°18 (one arrow) and n°28 (two arrows). B. Sagittal view. ST (arrow) of supplemental shape, impacted, and at the middle third of the adjacent roots of teeth n°13 and n°14. C. Coronal view. ST (arrow) impacted, and inclined toward the palatal side.

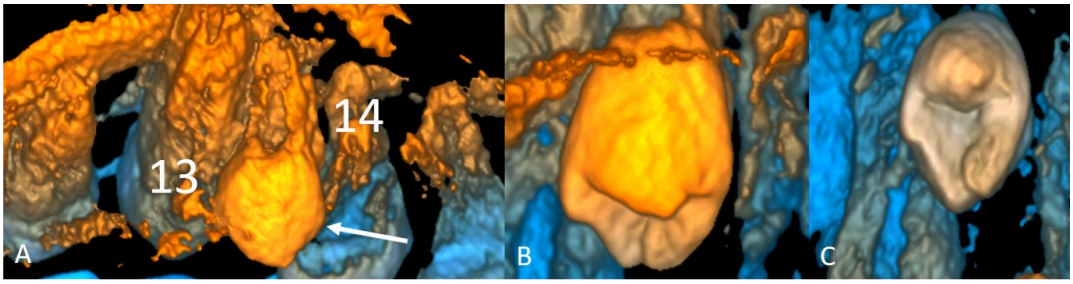

Fig. 23. Patient n°8. Planmeca 3D Mid CBCT. A. 3D right palatine view. ST (arrow) of supplemental shape, and at the level of the middle third of the adjacent roots of teeth n°13 and n°14. B. Detail of the ST's crown from posterior view. Asymmetry of the anterior cusp. C. Detail of the ST dysmorphic crown from the occlusal view.

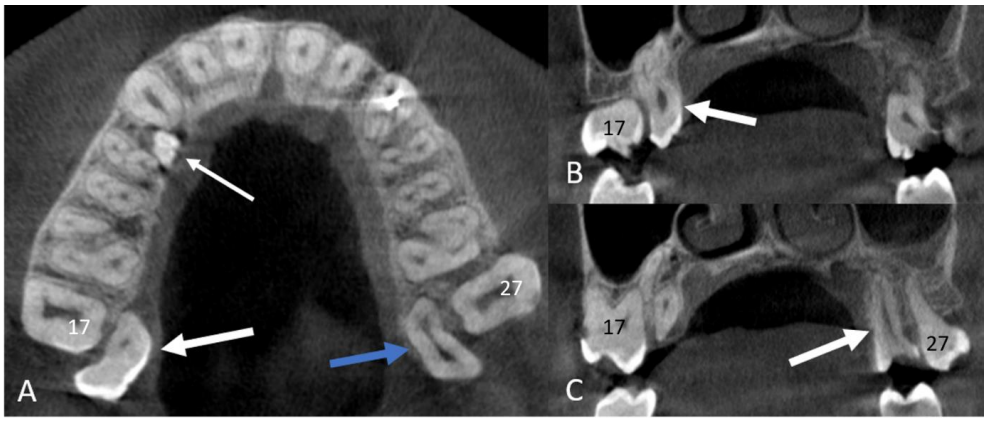

Fig. 24. Patient n°8. Planmeca 3D Mid CBCT. A. Axial view. ST (thin arrow). White thick arrow: dysmorphic tooth n°18 situated on the palatine side and palatine to the tooth n°17. Blue thick arrow: dysmorphic tooth n°28 situated on the palatine side and palatine to the tooth n°27. B. Coronal view. Tooth n°18 (arrow) palatine to tooth n°17 with roots surrounded by the right maxillary sinus. C. Coronal view. Tooth n°28 (arrow) palatine to tooth n°27, and without a relationship with the left maxillary sinus.

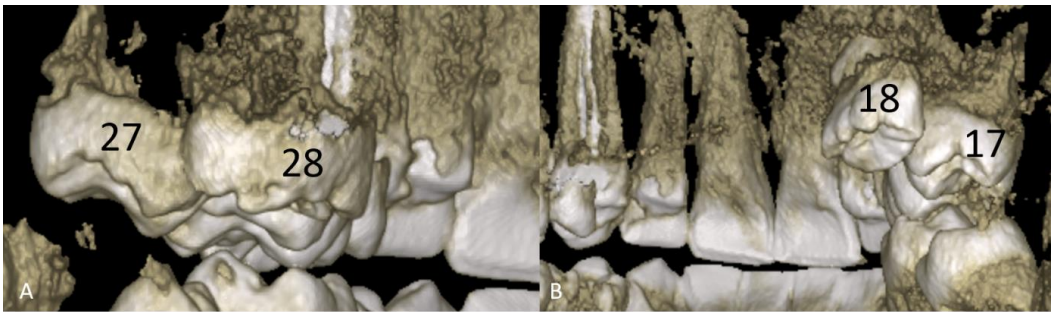

Fig. 25. Patient n°8. Planmeca 3D Mid CBCT. 3D posterior to anterior view of the maxilla. A. Left side. Dysmorphic tooth n°28 situated on the palatine side of the tooth n°27. B. Right side. Dysmorphic tooth n°18 situated on the palatine side of the tooth n°17.

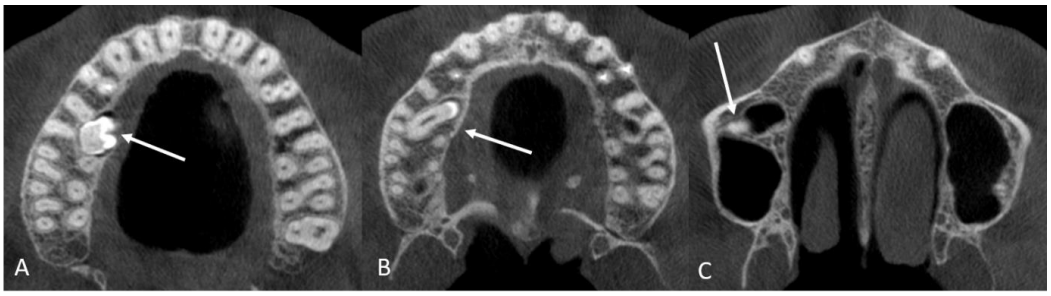

Fig. 26. Patient n°9. Planmeca 3D Mid CBCT. A. Axial view. ST (arrow) crown positioned on the right palatine side, between roots of teeth n°15 and n°16. B. Axial view. ST (arrow) is intra-alveolar, oblique, with the root of ST positioned between the roots of the tooth n°16. No signs of external resorption of the roots of the tooth n°16 by ST. C. Axial view. ST root apex (arrow) situated in the right transverse maxillary septum.

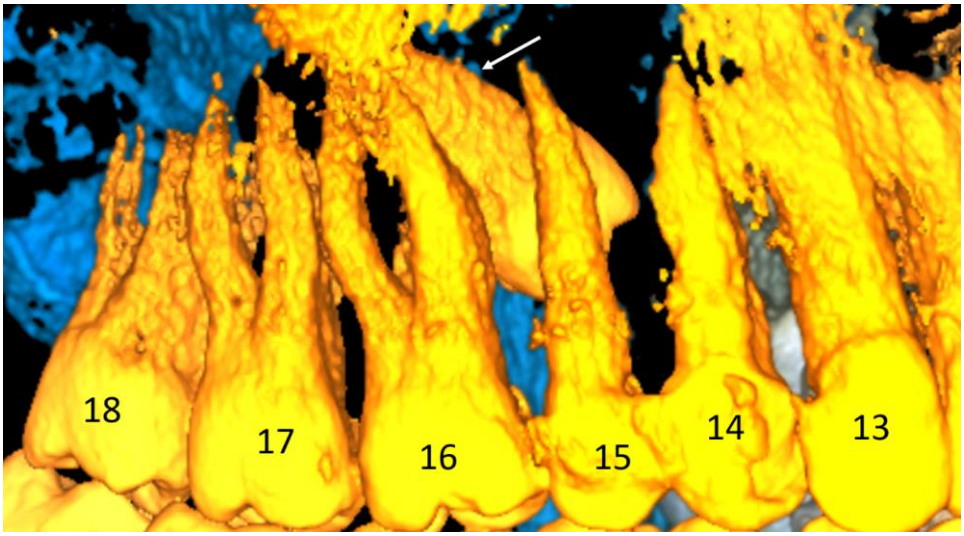

Fig. 27. Patient n°9. Planmeca 3D Mid CBCT. 3D lateral vestibular view of the right maxilla. ST (arrow) of supplemental shape, impacted, inclined toward the palatine side, and toward the midsagittal plane. The cusp of ST is located at the middle third of the tooth n°15.

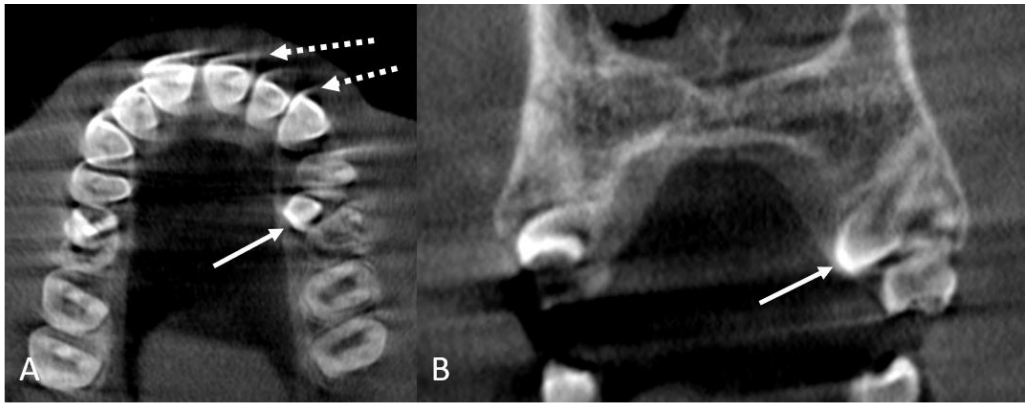

Fig. 28. Patient n°10. Planmeca 3D Mid CBCT. A. Axial view. ST (arrow) positioned on the left palatine side, between roots of teeth n°24 and n°64. Patient presents a movement artifact (arrows with dashes) with a rotation of the head from right to left during the scanning time [27]. B. Coronal view. ST (arrow) of supplemental shape, impacted, and inclined to the palatine side.

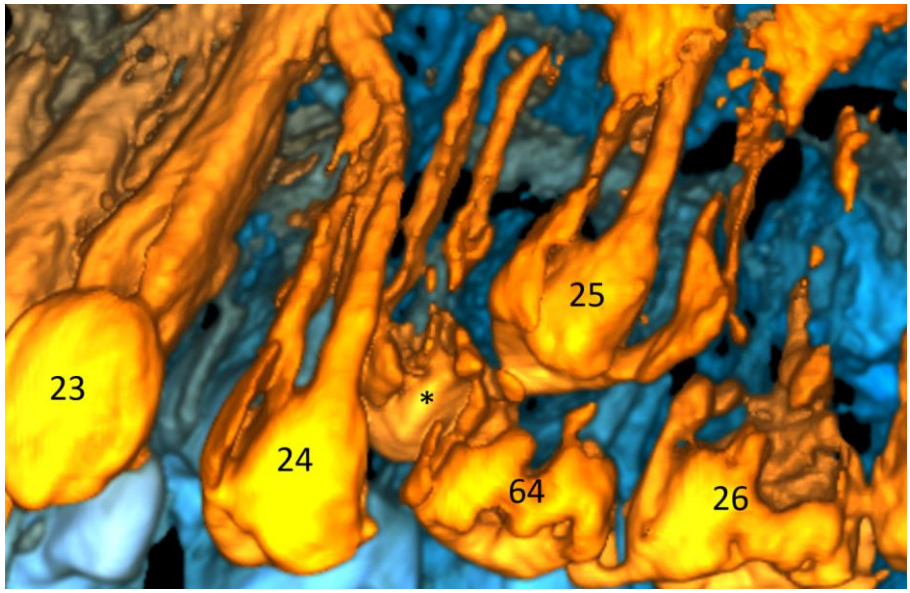

Fig. 29. Patient n°10. Planmeca 3D Mid CBCT. 3D lateral vestibular view of the left maxilla. ST (*) on the left palatine side, of supplemental shape, close to the cervical third of the root of the tooth n°24 and n°64.

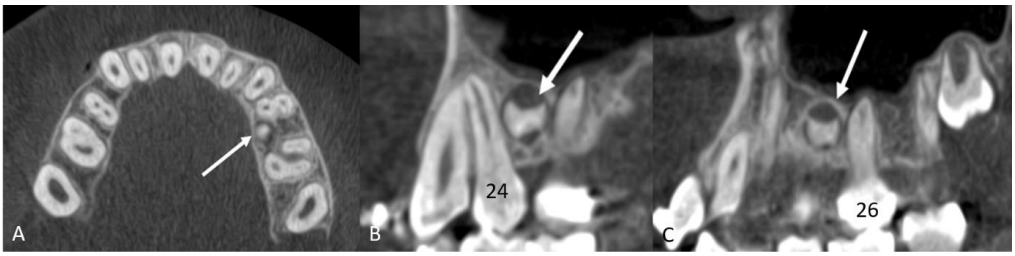

Fig. 30. Patient n°11. Planmeca 3D Mid CBCT. A. Axial view. ST (arrow) on the palatine side, and close to the tooth n°24. Absence of the tooth n°25. B. Sagittal view. ST (arrow) with the shape of a developing tooth bud, at the apical third of the adjacent root of tooth n°24. C. Sagittal view. ST (arrow) at the apical third of the adjacent mesiovestibular root of the tooth n°26.

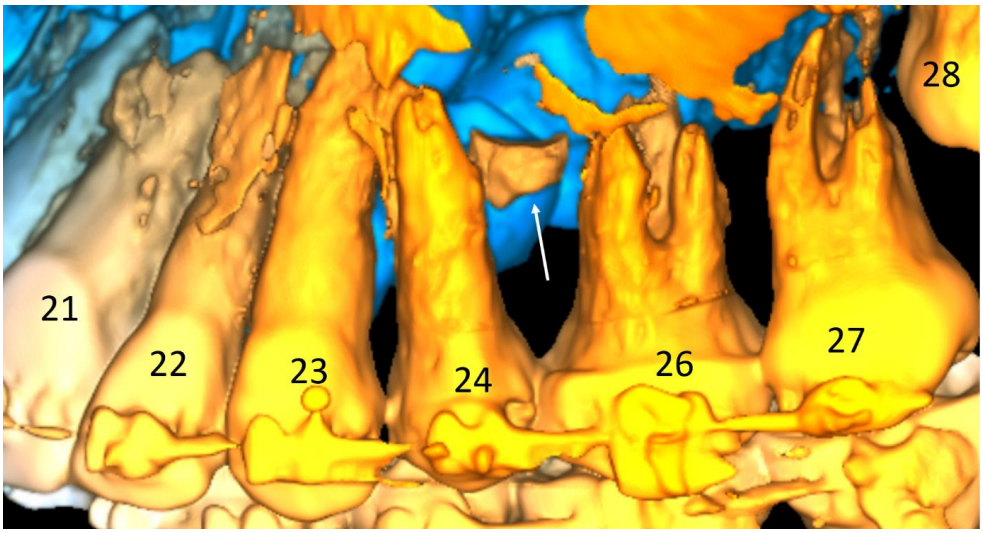

Fig. 31. Patient n°11. Planmeca 3D Mid CBCT. 3D lateral vestibular view of the left maxilla. ST (arrow) with the shape of a developing tooth bud at the apical third of the adjacent roots of teeth n°24 and n°26. Absence of the tooth n°25.

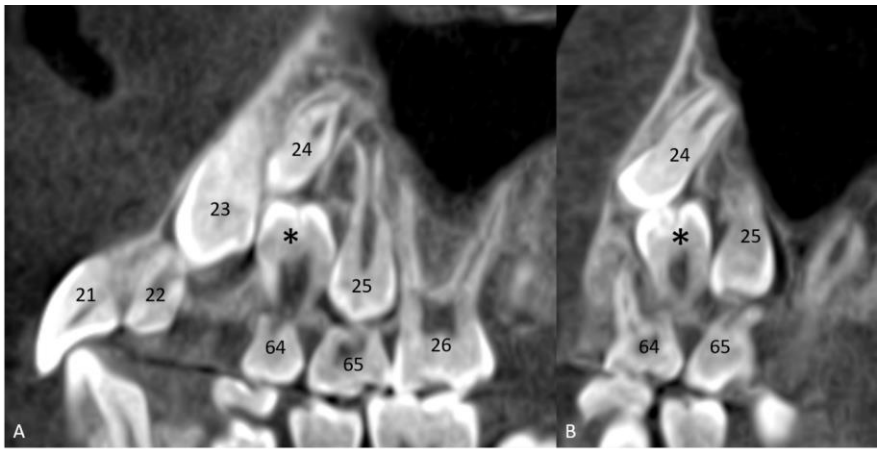

Fig. 32. Patient n°12. Planmeca 3D Mid CBCT. A. Reformatted sagittal view. ST (*) inverted, impacted, between the tooth n°64, and the tooth n°24. B. Reformatted sagittal view. ST (*) inverted, and of molariform shape. Occlusal contact between ST and the tooth n°24. Contact between the root of ST and the crown of the tooth n°25.

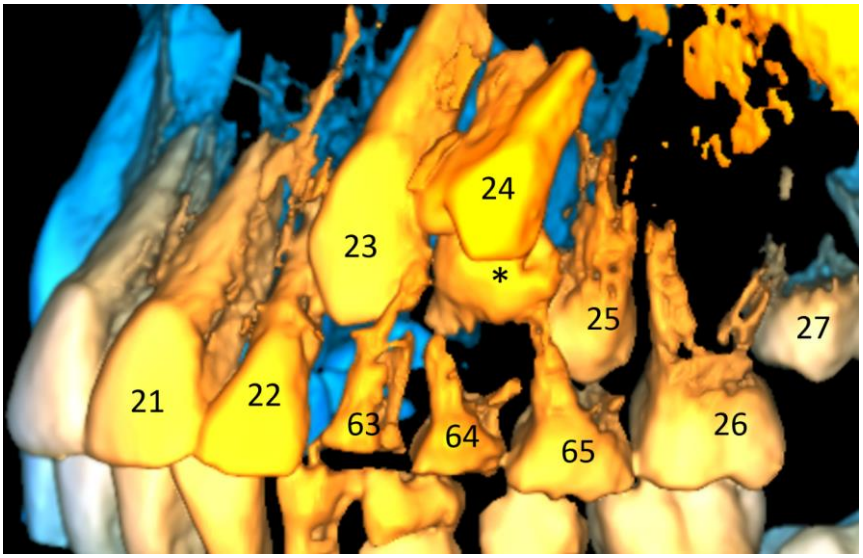

Fig. 33. Patient n°12. Planmeca 3D Mid CBCT. 3D lateral vestibular view of the left maxilla. ST (*) impacted, inverted, molariform, within the arch, between teeth n°24 (apical) and n°64 (occlusal). Tooth n°24 is inclined, displaced to the vestibule and with rotation: the mesial side of the tooth n°24 is oriented to the left vestibule.

3. Unilateral undersized supernumerary teeth

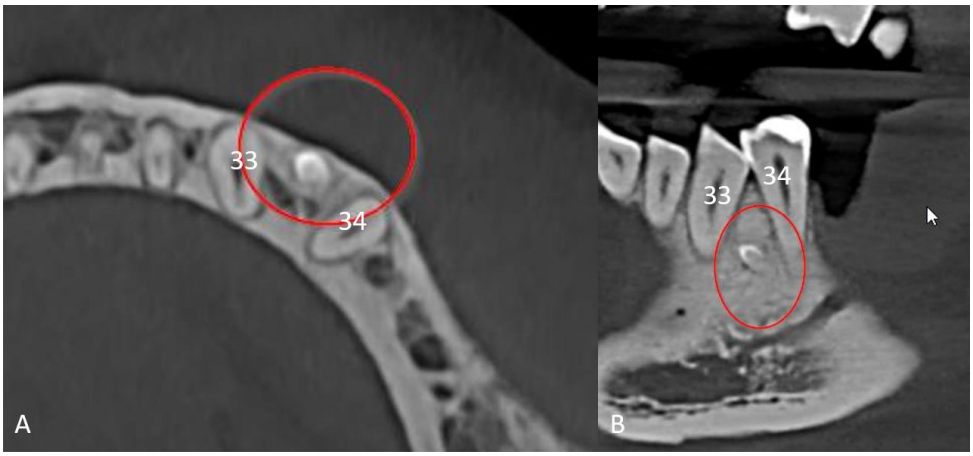

Fig. 34. Patient n°13. Carestream 9600 CBCT. A. Axial view. Conical, impacted, vestibular, undersized ST (inside the circle), between teeth n°33 and n°34. Rotation of the tooth n°33 to the mesial side. B. Sagittal view. Conical ST (inside the circle) impacted, inclined, at the apical third of the adjacent roots of teeth n°33 and n°34.

Fig. 35. Patient n°14. Planmeca 3D Mid CBCT. A. Axial view. ST (arrow) impacted, within the arch, between the teeth n°43 and n°44. B. Sagittal view. ST (arrow) impacted, vertical, at the apical third of the adjacent root of the tooth n°43. C. Coronal view. ST (arrow) impacted, vertical, at the apical third of the adjacent root of the tooth n°44.

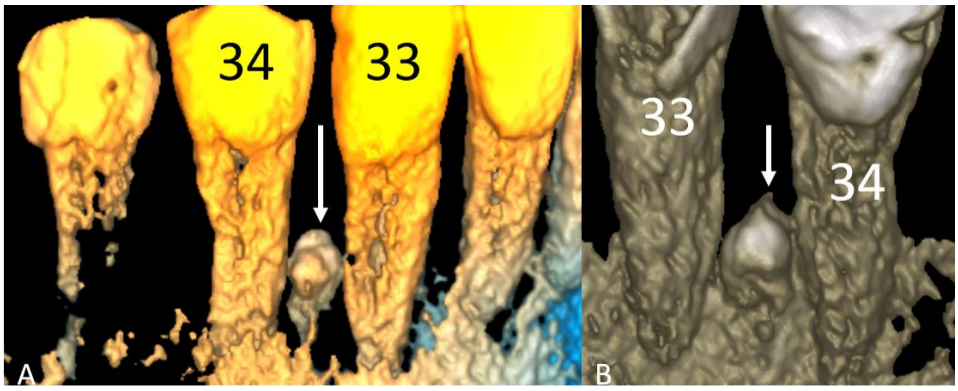

Fig. 36. Patient n°14. Planmeca 3D Mid CBCT. A. 3D vestibular view of the left mandible. Conical ST (arrow), impacted, vertical, at the apical third of the adjacent roots of the teeth n°33 and n°34. B. 3D lingual view of the left mandible. Molariform ST (arrow), impacted, vertical, at the apical third of the adjacent roots of the teeth n°33 and n°34.

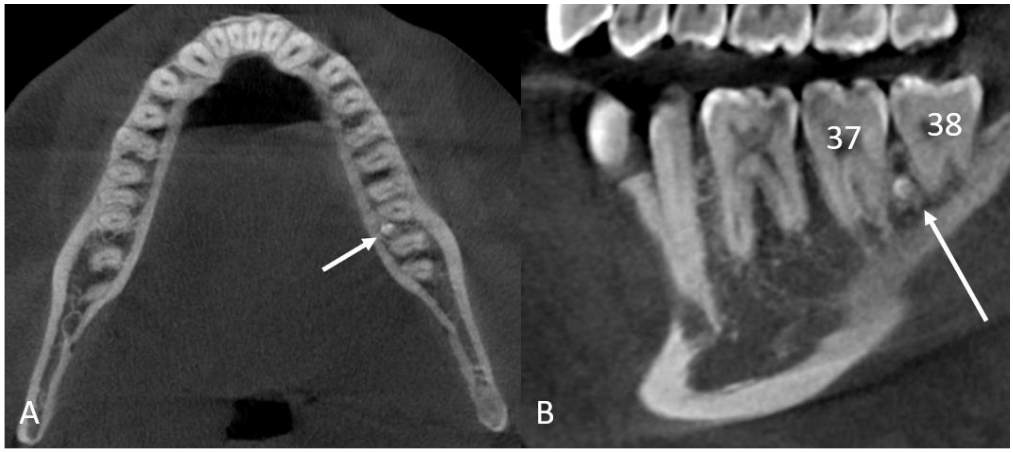

Fig. 37. Patient n°15. Planmeca 3D Mid CBCT. ST (arrow) on the lingual side, impacted, between the distal root of the tooth n°37, and the mesial root of the tooth n°38. B. ST (arrow) impacted, vertical, conical, undersized, at the apical third of the adjacent roots, and between the distal root of the tooth n°37, and the mesial root of the tooth n°38.

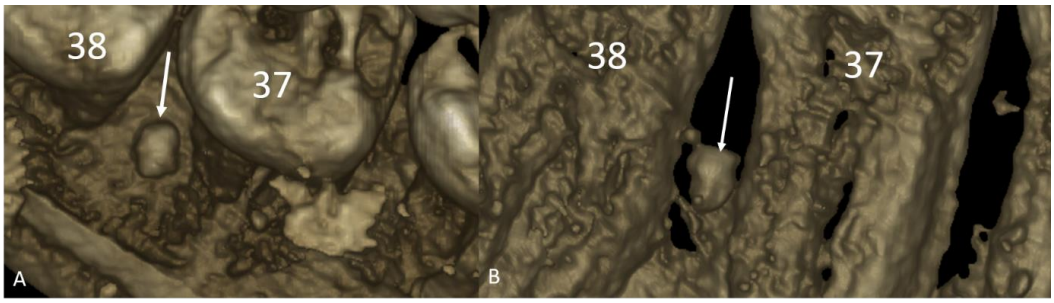

Fig. 38. Patient n°15. Planmeca 3D Mid CBCT. A. 3D occlusal and lingual view of the left mandible. Conical ST (arrow) between the teeth n°37 and n°38. B. 3D lingual view of the left mandible. Conical ST (arrow), between the teeth n°37 and 38, and at the middle third of the adjacent roots of teeth n°37 and n°38.

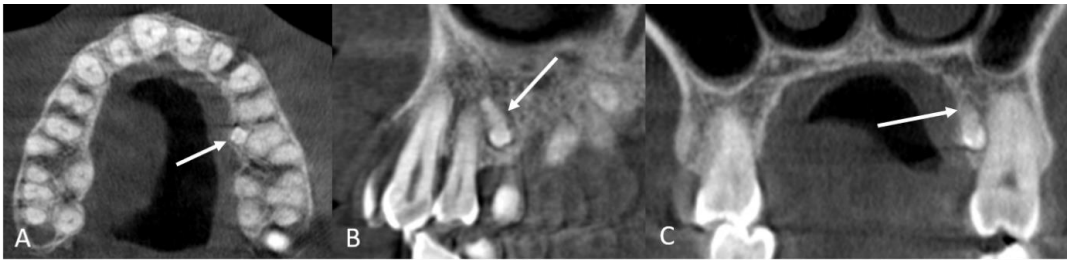

Fig. 39. Patient n°16. Planmeca 3D Mid CBCT. A. Axial view. ST (arrow) on the left palatine side, between the teeth n°24 and n°25. B. Sagittal view. Conical, inclined, and impacted ST (arrow), at the apical third of the adjacent root of the tooth n°24. C. Coronal view. Conical, impacted, ST (arrow) on left palatine side, and at the middle third of the adjacent root of the tooth n°25.

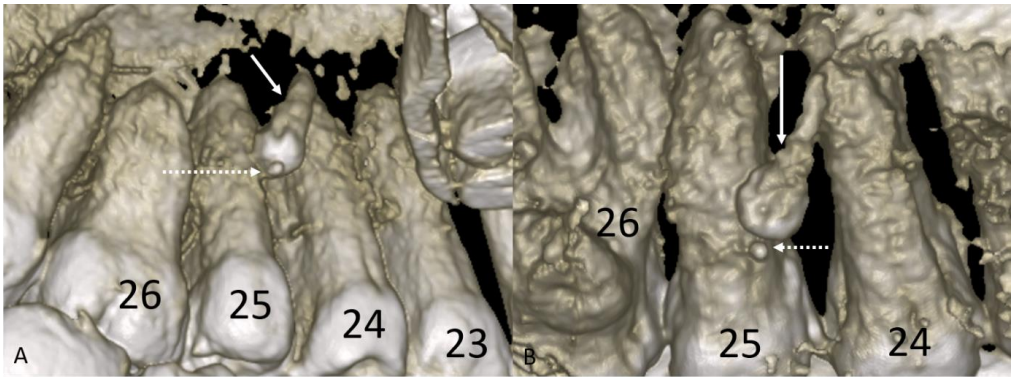

Fig. 40. Patient n°16. Planmeca 3D Mid CBCT. A. 3D lateral and upward view of the left maxilla. Conical ST (arow) on palatine side of the teeth n°24 and n°25. Dashed arrow: enamel pearl close to the ST's crown. B. 3D lateral view of the left maxilla. Conical ST (arrow) inclined to the distal side. Dashed arrow: enamel pearl close to the tip of the ST crown.

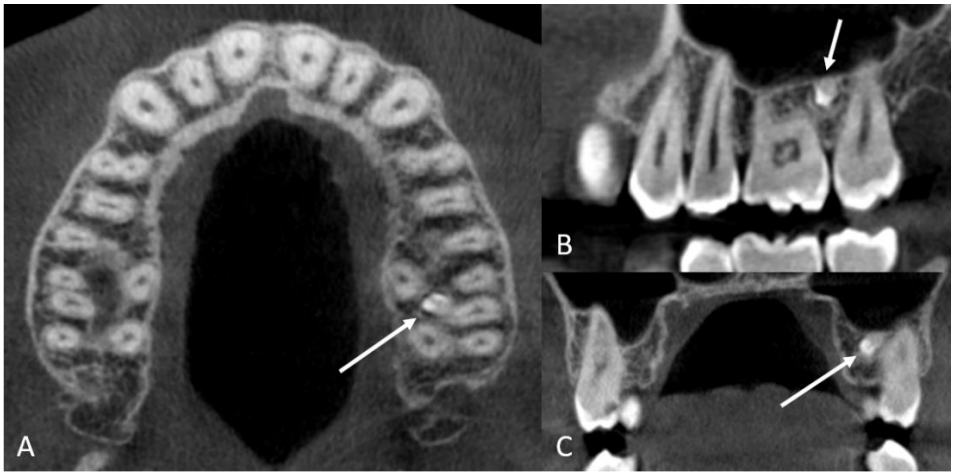

Fig. 41. Patient n°17. Planmeca 3D Mid CBCT. A. Axial view. Undersized ST (arrow) within the arch, between the roots of the teeth n°26 and n°27. B. Sagittal view. Undersized, conical ST (arrow), close to the floor of the left maxillary sinus. C. Coronal view. Undersized conical ST (arrow) inclined to the palatine side.

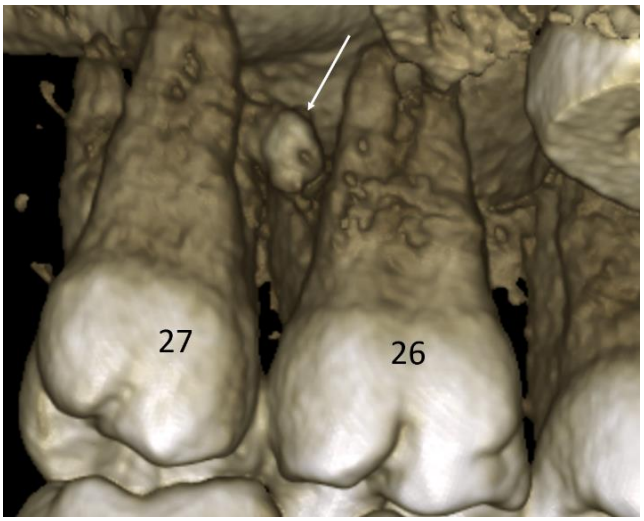

Fig. 42. Patient n°17. Planmeca 3D Mid CBCT. 3D lateral and upward view of the left maxilla. Undersized, conical, inclined ST (arrow), at the apical third of the adjacent roots of the teeth n°26 and n°27.

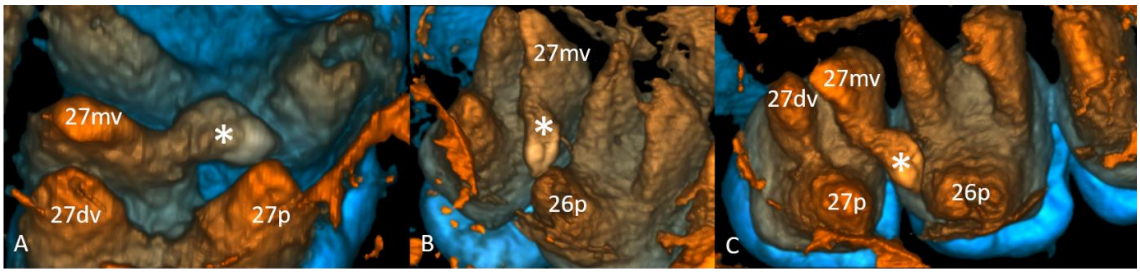

Fig. 43. Patient n°17. Planmeca 3D Mid CBCT. A. 3D view of the apex of the roots of the tooth n°27. Undersized conical ST (*) with the root positioned between mesiovestibular and palatine root of the tooth n°27. B. 3D view of the apex of the roots of the teeth n°26 and n°27. ST (*) with oblique orientation between the mesiovestibular root of the tooth n°27 and the palatine root of the tooth n°26. C. 3D view of the apex of the roots of the teeth n°26 and n°27. Conical undersized ST (*) with oblique orientation between the mesiovestibular root of the tooth n°27 and the palatine root of the tooth n°26.

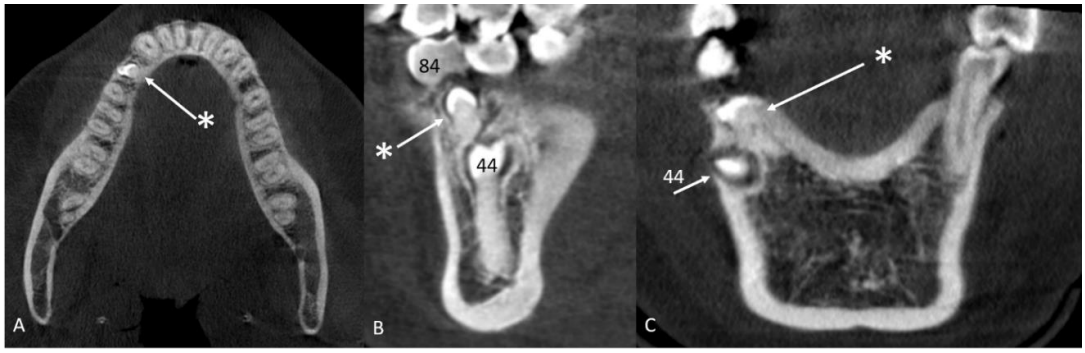

Fig. 44. Patient n°18. Planmeca 3D Mid CBCT. A. Axial view. ST (*) within the arch, between the roots of the teeth n°84 and n°44. B. Sagittal view. Conical ST (*) under the crown of the tooth n°84, and apical to the crown of the tooth n°44. C. Coronal view. Conical impacted ST (*) inclined to vestibular side. Crown of the tooth n°44 (arrow) impacted and perforating the cortical vestibular bone.

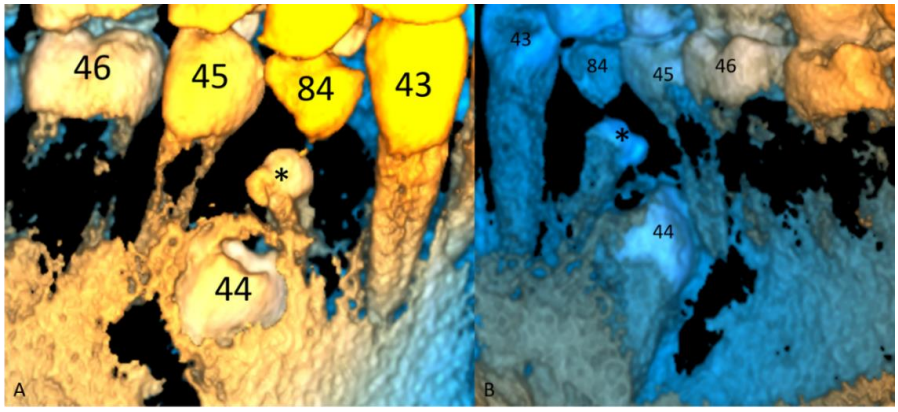

Fig. 45. Patient n°18. Planmeca 3D Mid CBCT. A. 3D lateral vestibular view of the right mandible. Conical ST (*) positioned between teeth n°84 and n°44. Tooth n°44 impacted, in rotation, with its mesial side oriented to the right vestibule. B. 3D lateral lingual view of the right mandible. Conical impacted ST (*) between teeth n°84 and n°44. Tooth n°44 inclined to the distal side, and close to the apical third of the root of the tooth n°45.

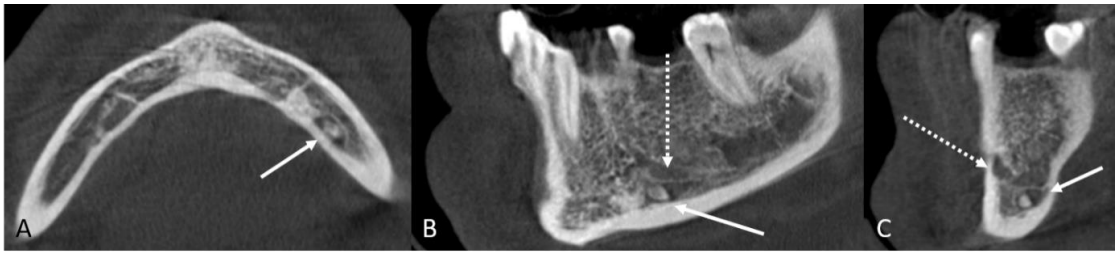

Fig. 46. Patient n°19. Planmeca 3D Mid CBCT. A. Axial view. Undersized ST (arrow) close to the left lingual cortical bone. B. Parasagittal view through the ST. Horizontal undersized ST (arrow) oriented to the distal side and positioned under the left inferior alveolar nerve canal (arrow with dashes). C. Parasagittal view through the ST. Undersized ST (arrow) with follicle under the left inferior alveolar nerve (arrow with dashes).

4. Bilateral supernumerary teeth

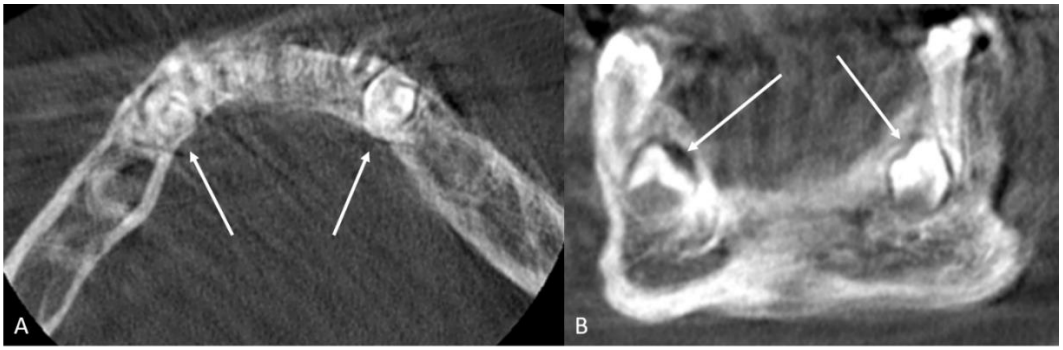

Fig. 47. Patient n°20. Planmeca 3D Mid CBCT. A. Axial view. Bilateral ST (arrows) within the arch, between the roots of the teeth n°43 and n°44, and between teeth n°33 and n°34. Degradation of the quality of the image due to the artifact of movement [27]. B. Coronal view. Impacted bilateral ST (arrows) with the shape of a developing tooth bud at the apical third of the adjacent roots of the teeth n°44 and n°34.

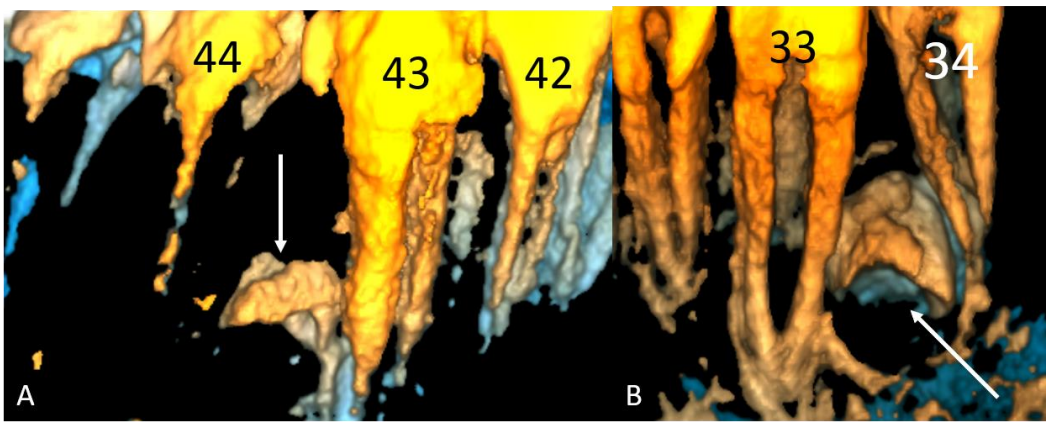

Fig. 48. Patient n°20. Planmeca 3D Mid CBCT. A. 3D vestibular lateral view of the right mandible. A developing tooth bud ST (arrow) between the roots of the teeth n°43 and n°44. ST is close to the apical third of the adjacent root of the tooth n°43. B. 3D vestibular lateral view of the left mandible. A developing tooth bud ST (arrow) between the roots of teeth n°33 and n°34. ST (arrow) is close to the middle third of the adjacent root of the tooth n°33, and to the apical third of the adjacent root of the tooth n°34.

Fig. 49. Patient n°21. Planmeca 3D Mid CBCT. A. Axial view at the level of the cusps of ST crowns. Molariform bilateral ST (arrows) on the lingual side between the roots of the teeth n°43 and n°44, and between the teeth n°33 and n°34. B. Axial view at the level of crowns of ST (arrows). Molariform impacted ST (arrow) close to the lingual root of the tooth n°44. Molariform impacted ST (arrow) close to the root of the tooth n°34. C. Axial view at the level of the ST's roots. Inclined ST on the lingual side of the tooth n°33 (arrow). Vertical and rotated ST lingual to the root of the tooth n°33 (arrow).

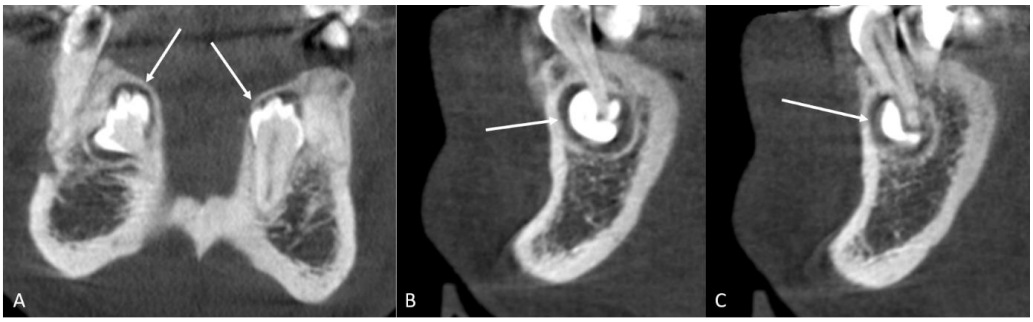

Fig. 50. Patient n°21. Planmeca 3D Mid CBCT. A. Coronal view. Inclined, impacted, lingual, molariform ST (arrow) on the right side. Vertical, impacted, lingual, molariform ST (arrow) on the left side. B. Left sagittal view. Crown of ST (arrow) around the apex of the tooth n°34. C. Right sagittal view. Resorption of the apical third of the root of the tooth n°44 by ST crown (arrow).

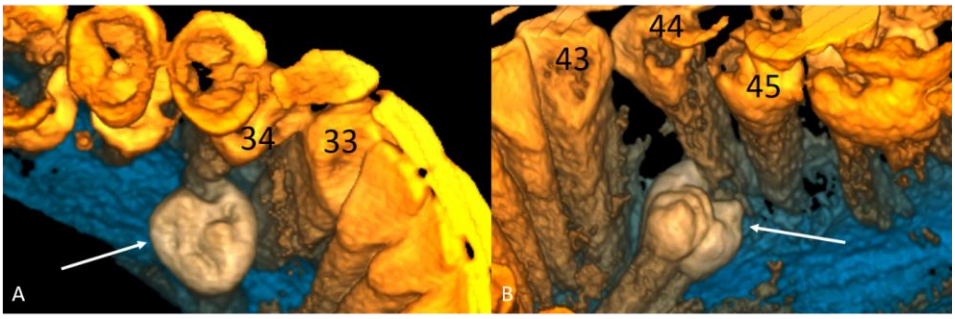

Fig. 51. Patient n°21. Planmeca 3D Mid CBCT. 3D occlusal and lingual view of the left mandible. Molariform ST (arrow) with the crown surrounding the apex of the tooth n°34. B. 3D lateral lingual view of the right mandible. ST (arrow) inclined toward distal side with the resorption of the apical third of the root of the tooth n°44.

Fig. 52. Patient n°22. Planmeca 3D Mid CBCT. A. Axial view. ST on the lingual side between the teeth n°33 and n°34, and between the teeth n°43 and 44. B. Coronal view. Right molariform, impacted, vertical ST (thin arrow) lingual to the tooth n°44. ST is present at to the middle third of the adjacent root of the tooth n°44. Left molariform, impacted, inclined to vestibular side ST (thick arrow) close to the middle third of the adjacent root of the tooth n°34. Dilaceration of the root of the tooth n°34.

5. Additional features

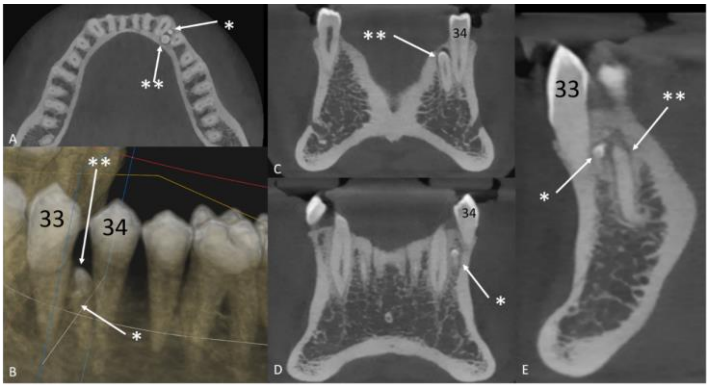

Fig. 53. Patient n°23. Carestream 9600 CBCT. A. Axial view. Undersized ST (*) on vestibular side, and additional ST (**) on the lingual side between the roots of the teeth n°33 and n°34. B. 3D lateral vestibular view of the left mandible. Undersized vertical ST (*) on vestibular side and additional conical ST (**) on lingual side between roots of the teeth n°33 and n°34. C. Coronal view through the conical ST (**). Conical ST (**) impacted, vertical, lingual, and close to the middle third of the adjacent root of the tooth n°34. D. Coronal view through the undersized ST (*). Undersized ST (*) impacted, vertical, close to the middle third of the adjacent root of the tooth n°33. E. Parasagittal view through both of ST. Undersized, vestibular ST (*) close to the middle third of the adjacent root of the tooth n°33. Conical ST (**) on the lingual side with dilacerated root.

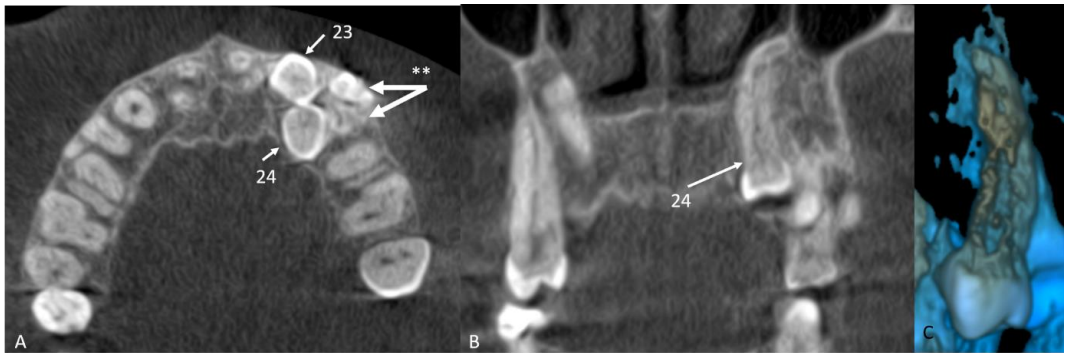

Fig. 54. Patient n°24. Planmeca 3D Mid CBCT. A. Axial view. Compound odontoma (**) on vestibular side between the teeth n°23 (mesial), n°24 (palatine), and n°25 (distal). B. Coronal view. Tooth n°24 displaced on palatine side. The root of the tooth n°24 is dilacerated. C. 3D view of the dilacerated tooth n°24.

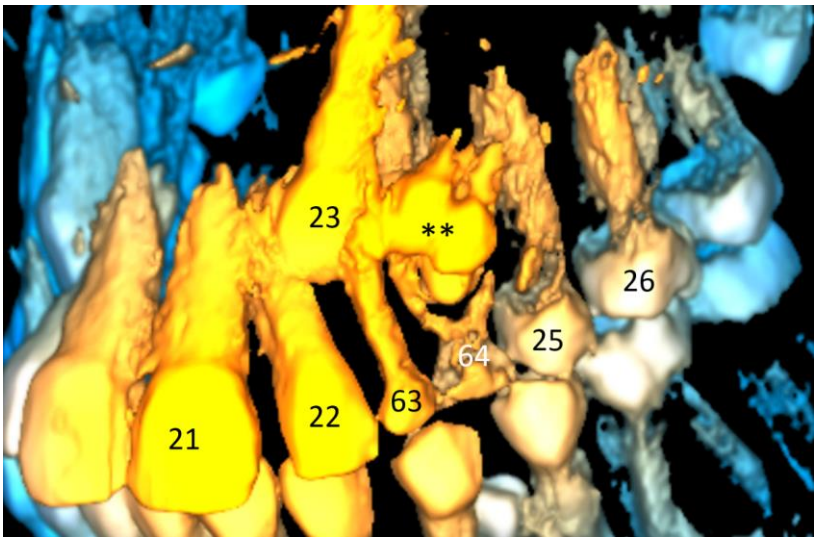

Fig. 55. Patient n°24. Planmeca 3D Mid CBCT. 3D lateral and vestibular view of the left mandible. Compound odontoma (**) on vestibular side and apical to the tooth n°64.

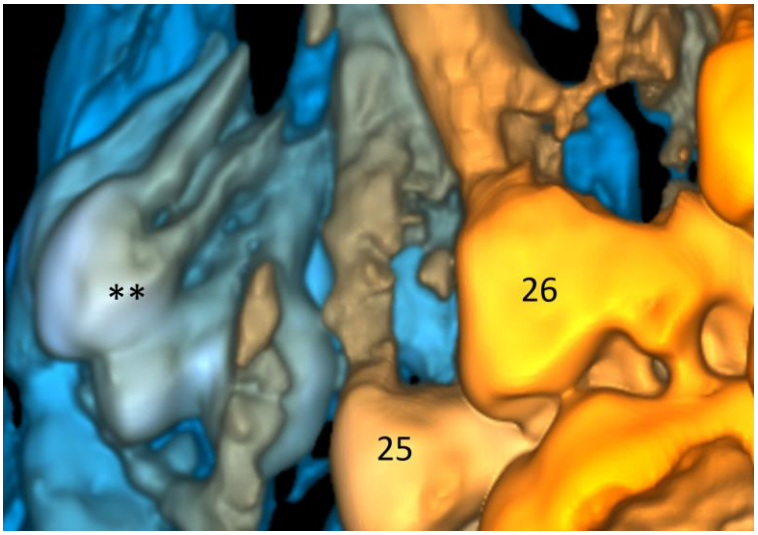

Fig. 56. Patient n°24. Planmeca 3D Mid CBCT. 3D lateral and posterior-anterior vestibular view of the left mandible. Compound odontoma (**) inclined and vestibular to the adjacent tooth n°25.

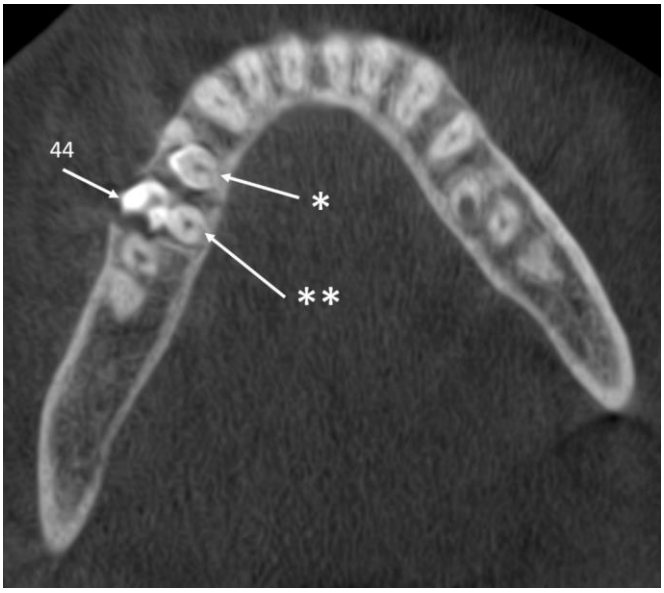

Fig. 57. Patient n°24. Planmeca 3D Mid CBCT. Two ST at the level of the tooth n°84 (*) and lingual to the tooth n°44 (**).

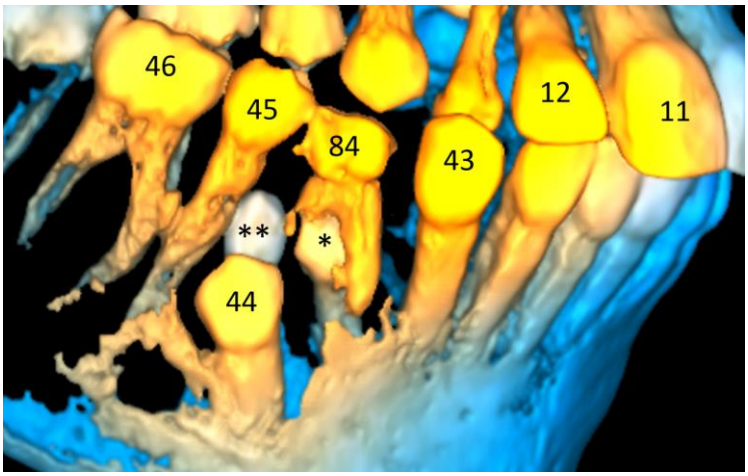

Fig. 58. Patient n°24. Planmeca 3D Mid CBCT. 3D lateral vestibular view of the right mandible. Conical ST (*) inside the roots of the tooth n°84. ST (**) impacted, vertical, lingual to the tooth n°44, and close to the middle third of the adjacent root of the tooth n°45. Tooth n°44 is impacted, vestibular, and inclined to the distal side.

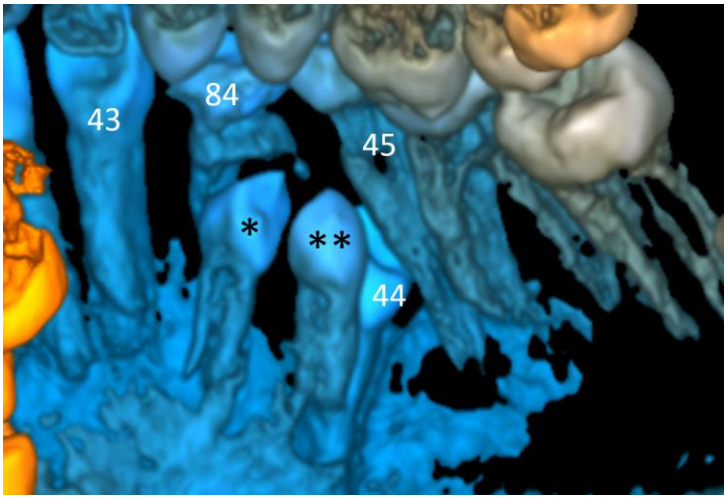

Fig. 59. Patient n°24. Planmeca 3D Mid CBCT. 3D lateral lingual view of the right mandible. Conical, vertical, lingual ST (*) between the roots of the tooth n°84. ST (*) with rotation with its distal side oriented to the vestibule. Conical, vertical ST (**), and lingual to the tooth n°44.

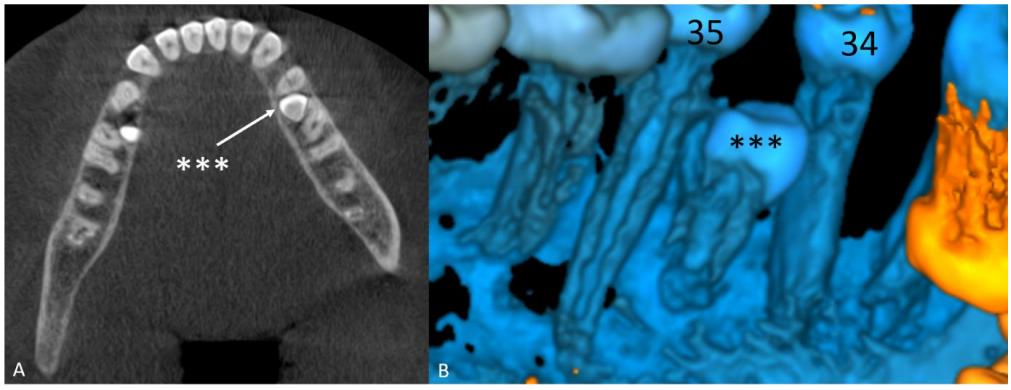

Fig. 60. Patient n°24. Planmeca 3D Mid CBCT. ST (***) within the arch, and between the roots of the teeth n°34 and n°35. B. 3D lateral lingual view of the left mandible. Supplemental ST (***) close to the middle third of the adjacent root of the tooth n°34 and n°35.

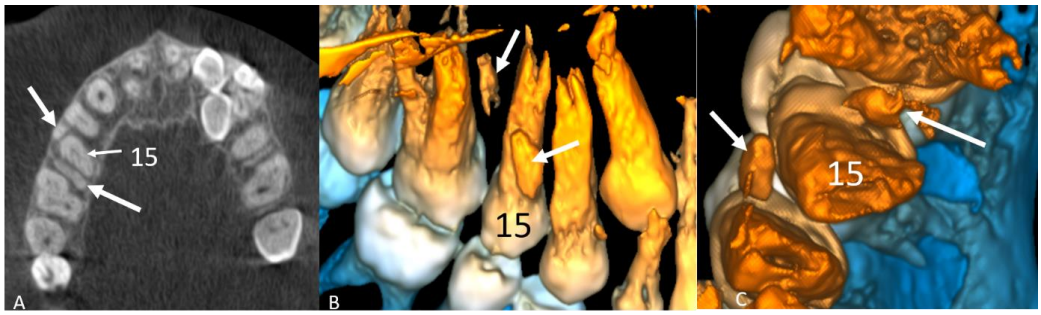

Fig. 61. Patient n°24. Planmeca 3D Mid CBCT. A. Axial view. Remnants (arrows) of the roots of the tooth n°55. B. 3D vestibular view of the right maxilla. Mesiovestibular and distal remnants (arrows) of the roots of the tooth n°55. C. 3D apical view of roots apices of the right maxilla. Mesiovestibular and distal remnants (arrows) of the roots of the tooth n°55.

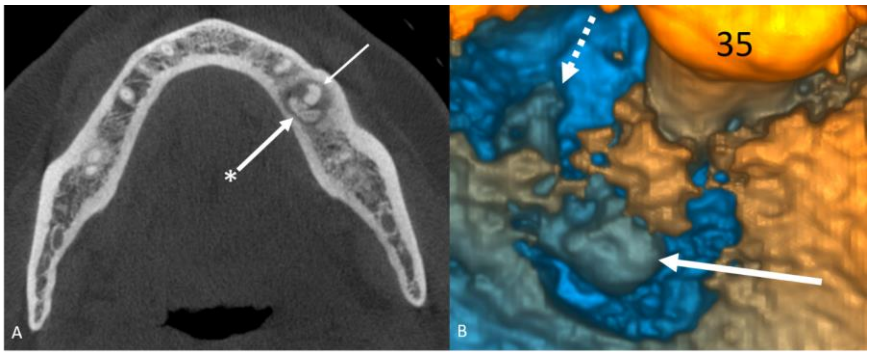

Fig. 62. Patient n°25. Planmeca 3D Mid CBCT. A. Axial view. Horizontal ST (*) on lingual side, and around the apex of the tooth n°35. ST (*) and the apex of the tooth n°35 are surrounded by an osteolytic cystic-like lesion. B. 3D lateral lingual view of the surroundings of the tooth n°35. Crown of ST (arrow), and apex of the ST (arrow with dashes).

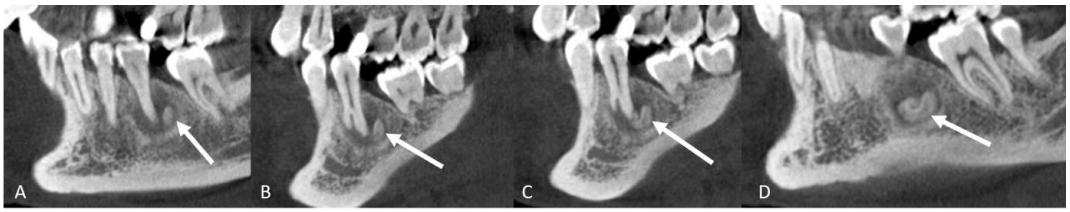

Fig. 63. Patient n°25. Planmeca 3D Mid CBCT. Parasagittal view through the ST (arrow) and the apex of the taurodontic tooth n°35. A. Vestibular view. B. Anterior intra-alveolar view. C. Posterior intra-alveolar view. D. Lingual view. ST with dilacerated root.

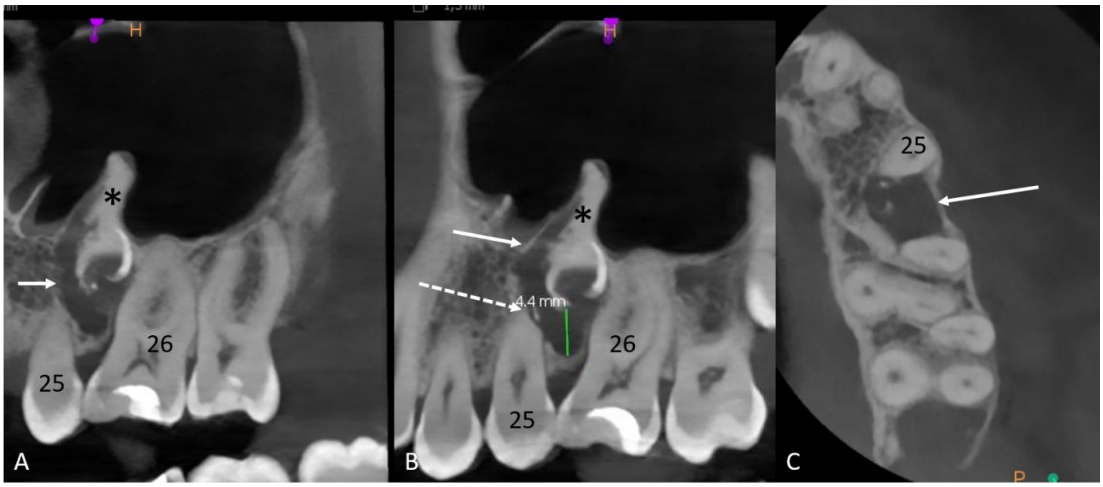

Fig. 64. Patient n°26. Carestream 9600 CBCT. A. Sagittal view. Vertical supplemental ST (*) between the teeth n°25 and n°26. Dentigerous cyst (arrow) around ST (*). The root of ST (*) is surrounded by the left maxillary sinus. External resorption of the crown and of the root of ST (*) by the dentigerous cyst. B. Sagittal view. External resorption of the root of the tooth n°25 (arrow with dashes). Dentigerous cyst (arrow) around ST (*). C. Axial view. External resorption of the root of the tooth n°25. Thinning of the vestibular cortical bone (arrow).

6. Major hyperdontia

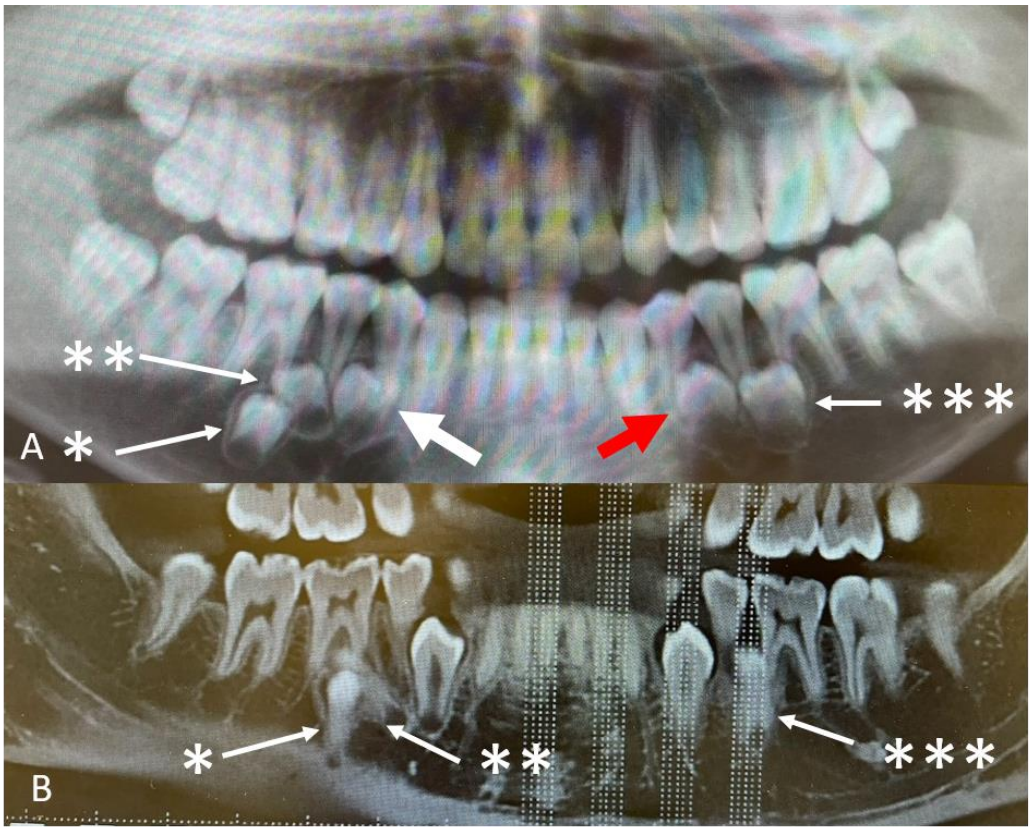

Fig. 65. Patient n°27. A. Panoramic X-ray. Developing tooth bud ST (*) apical to the tooth n°46. Developing tooth bud ST (**) apical to the teeth n°46 and n°45. Developing tooth bud ST (thick white arrow) between the teeth n°45 and n°44. Developing tooth bud ST (thick red arrow) between the teeth n°34 and n°35. Developing tooth bud ST (***) between the teeth n°35 and n°36. B. I-CAT CBCT. Pseudo-panoramic view of the mandible. Conical vertical ST (*) apical to the tooth n°46. Conical ST (**) inclined to the distal side. Conical vertical ST (***) close to the apical third of the mesial root of the tooth n°36.

Fig. 66. Patient n°28. Panoramic X-ray. Arrows: three impacted ST.

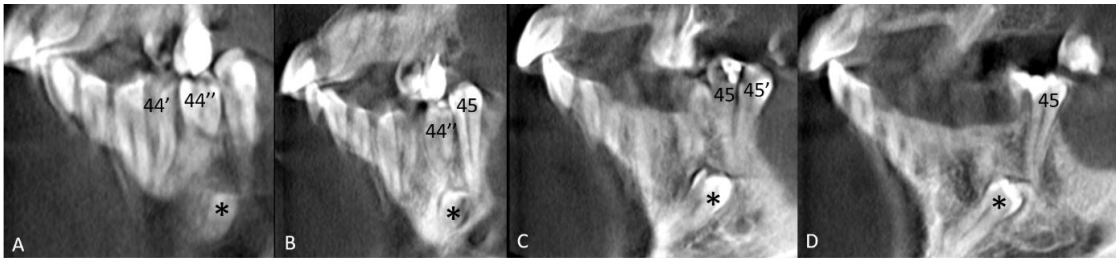

Fig. 67. Patient n°28. Planmeca 3D Mid CBCT. Reformatted parasagittal view. A. ST teeth n°44' and 44'' erupted and on the arch. Crown of the impacted tooth n°44 (*). B. ST tooth n°44''erupted and on the arch. Crown of the impacted tooth n°44 (*) with the contact with the apex of the tooth n°45, and without external resorption. C. ST tooth n°45' erupted, on the arch, and distal to tooth n°45. Crown of the tooth n°44 (*) at the apex of teeth n°45 and 45', and without external resorption. D. The tooth n°44 (*) impacted, and inclined at the apex of the tooth n°45.

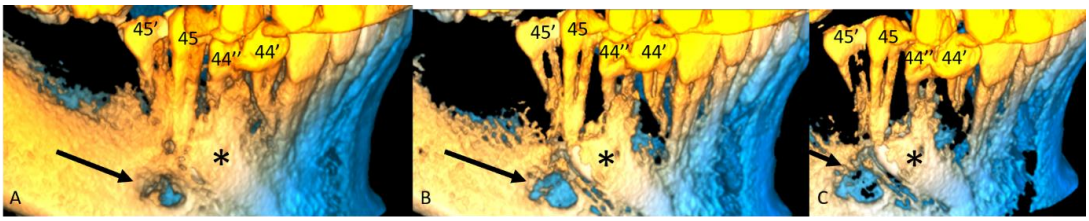

Fig. 68. Patient n°28. Planmeca 3D Mid CBCT. 3D lateral vestibular view of the right mandible. Progressive modification of the bone threshold. Anatomic topography of normal and ST teeth in the right premolar area. A. Black arrow: right foramen mentale. Tooth n°44 (*) under vestibular cortical bone. B. Black arrow: right foramen mentale. Tooth n°44 (*) with partially visible crown. C. Black arrow: right foramen mentale. Tooth n°44 (*) well visualized from the crown to the apex of the root. Tooth n°44 at a distance from the right foramen mentale.

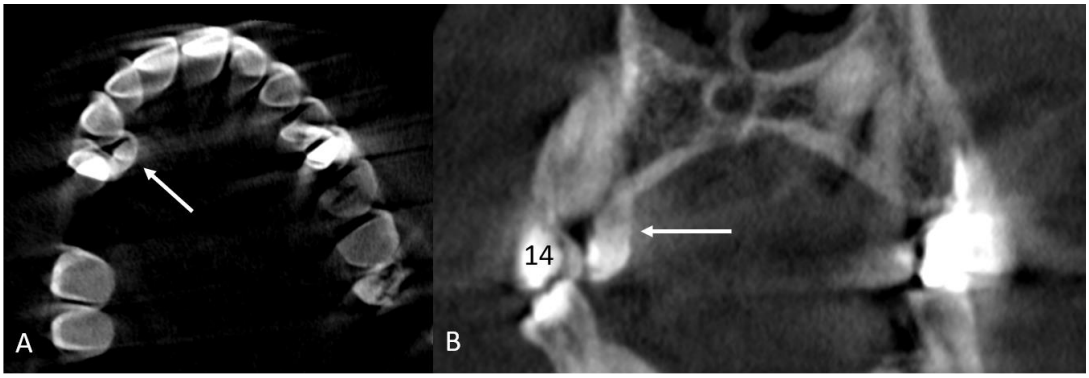

Fig. 69. Patient n°28. Planmeca 3D Mid CBCT. A. Axial view of the maxilla. Arrow: ST on the palatine side between teeth n°13 and n°14. B. Coronal view. Conical, impacted, and vertical ST palatine to the tooth n°14.

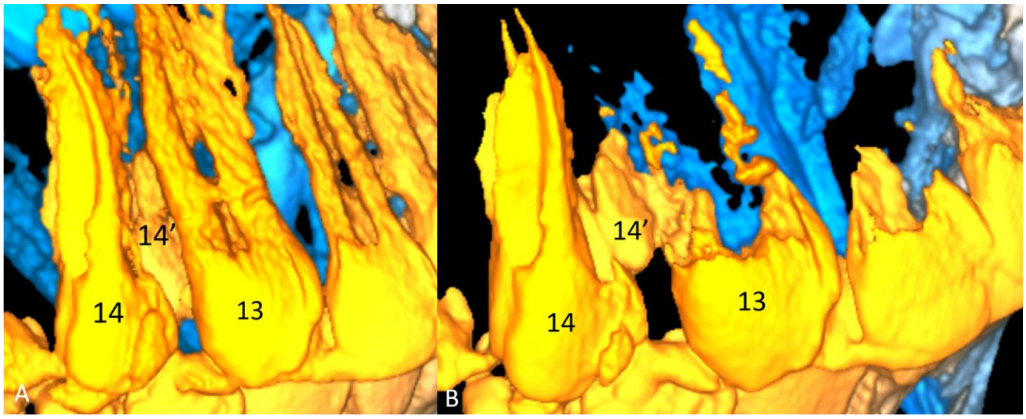

Fig. 70. Patient n°28. Planmeca 3D Mid CBCT. 3D lateral vestibular view of the right maxilla. Conical ST is palatine, and between the roots of the teeth n°13 and n°14. B. 3D lateral vestibular view of the right maxilla with modification of the bone threshold. Conical ST is positioned at the cervical third of the root n°14, on palatine side and mesial to the root of the tooth n°14.

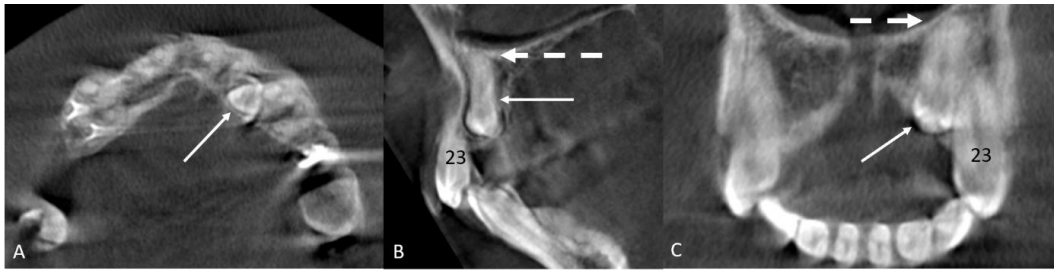

Fig. 71. Patient n°28. Planmeca 3D Mid CBCT. A. Axial view of the maxilla. Palatine ST between the teeth n°22 and n°23. B. Parasagittal view through the ST. ST (arrow) of supplemental shape, and palatine to the tooth n°23. Arrow with dashes: the apex of ST is localized within the floor of the left maxillary sinus. C. Coronal view through ST. ST of supplemental shape, vertical, at the middle third of the tooth n°23. Arrow with dashes: the apex of ST is localized within the floor of the left maxillary sinus.

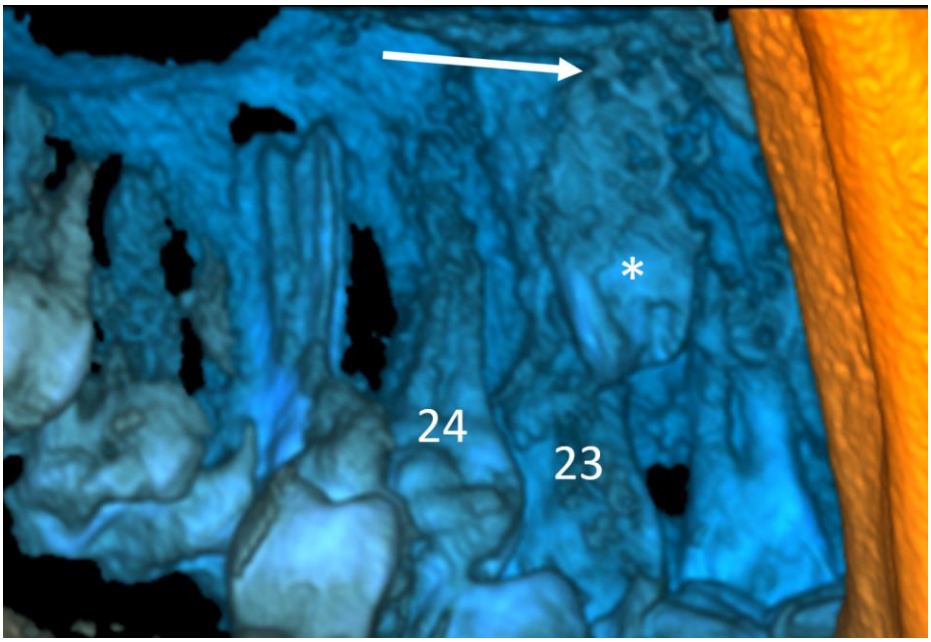

Fig. 72. Patient n°28. Planmeca 3D Mid CBCT. 3D palatine view of the left maxilla. ST of supplemental shape (*), and between the teeth n°23 and n°22. Arrow: the apex of ST is localized within the floor of the left maxillary sinus.

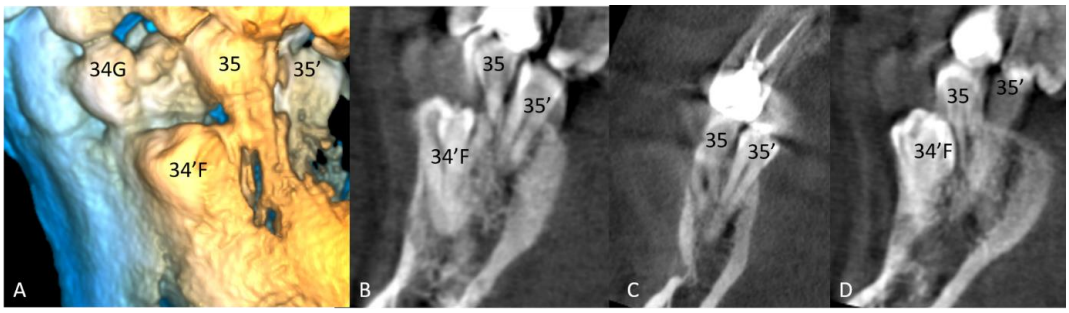

Fig. 73. Patient n°28. Planmeca 3D Mid CBCT. A. 3D lateral vestibular view of the left mandible. Tooth n°34G: gemination of the tooth n°34 which is erupted and in occlusion. ST tooth n°34'F (fusion) is vestibular, and impacted. Tooth n°35 is on the arch and in occlusion. Tooth n°35' of supplemental shape, coronal, and palatine to the tooth n°35. B-D: consecutive parasagittal views through teeth n°34'F, 35 and 35'. No external resorption of the tooth n°35 by teeth n°34'F and 35'.

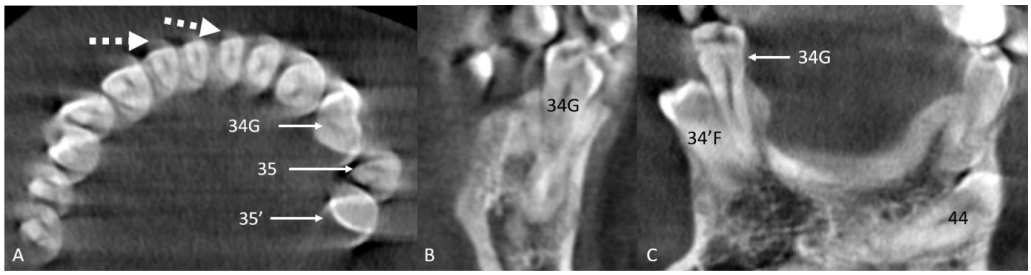

Fig. 74. Patient n°28. Planmeca 3D Mid CBCT. A. Axial view of the mandible. Double crown of the geminated tooth n°34G. Tooth n°35 is vestibular to the tooth n°35'. Dotted arrows: artifact of movement indicating the rotation of the head from left to right during the scanning time [27]. B. Parasagittal view through the geminated tooth n°34G. C. Coronal view of the tooth n°34G and 34'F inclined to vestibular side and with two roots. Tooth n°44 impacted and inclined to the vestibular side.

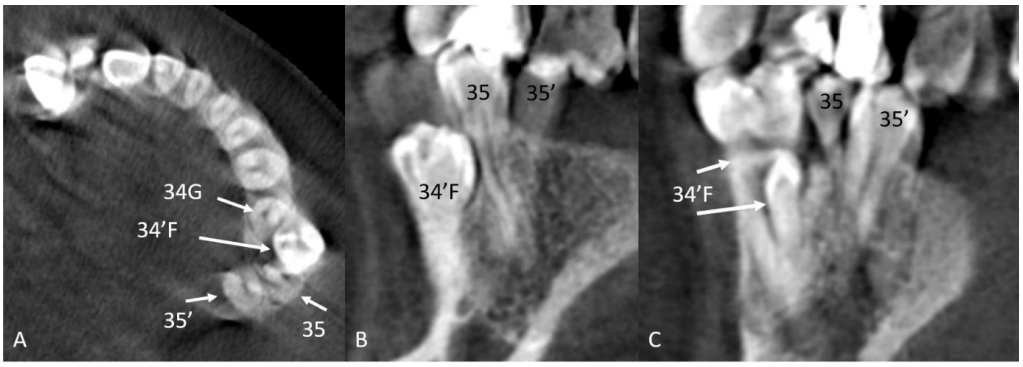

Fig. 75. Patient n°28. Planmeca 3D Mid CBCT. Planmeca 3D Mid CBCT. A. Reformatted axial view of the mandible. Topographic relationship between left premolars. B. Parasagittal view through 34'F, 35, and 35'. C. Tooth n°34'F is a fusion between a premolar of supplemental shape and a conical tooth on its lingual side.

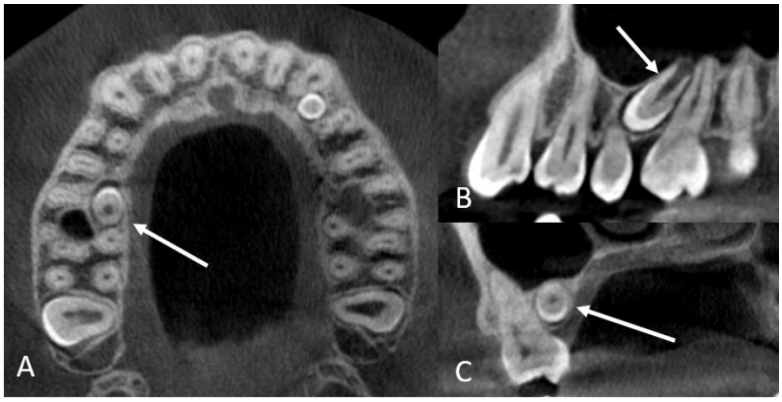

Fig. 76. Patient n°29. Planmeca 3D Mid CBCT. Axial view. ST n°1 (arrow) on lingual side of the right maxilla between the mesiovestibular and palatine root of the tooth n°16. B. Sagittal view. ST n°1 (arrow) with conical shape inclined toward the mesial side. The root of the ST n°1 is surrounded by the right maxillary sinus. ST n°1 is close to the middle third of the adjacent palatine root of the tooth n°16. C. Coronal view. ST n°1 (arrow) is palatine, horizontal, and close to the floor of the right maxillary sinus.

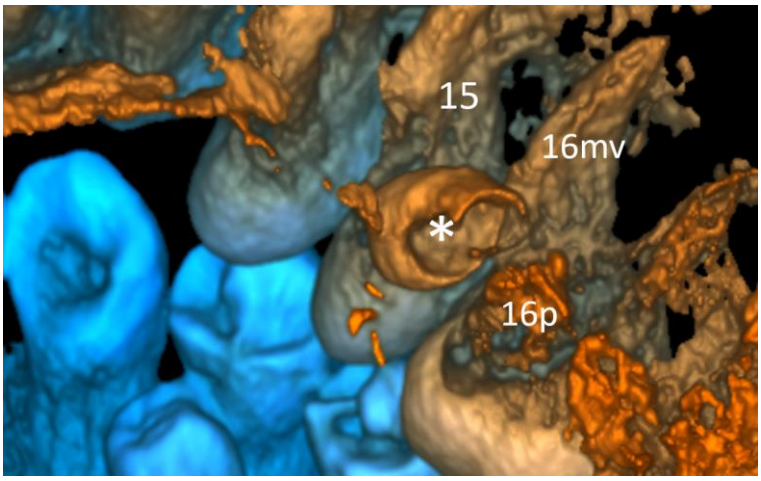

Fig. 77. Patient n°29. Planmeca 3D Mid CBCT. 3D view of apices of the teeth n°15 and 16. ST n°1 (*) palatine, with its root between the mesiovestibular and palatine root of the tooth n°16. ST n°1 (*) crown is oriented to caudal direction and to the root of the tooth n°15.

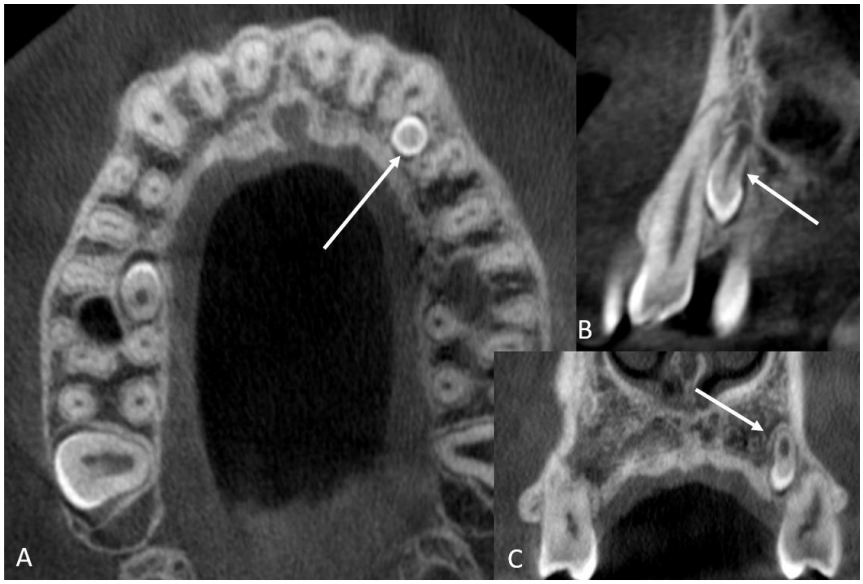

Fig. 78. Patient n°29. Planmeca 3D Mid CBCT. A. Axial view. ST n°2 (arrow) within the arch, and between the teeth n°23 and n°24. B. Sagittal view. Conical, impacted, vertical ST n°2 (arrow) close to the middle third of the root of the adjacent tooth n°23. C. Coronal view. Conical, vertical, palatine ST n°2 (arrow) close to the tooth n°24.

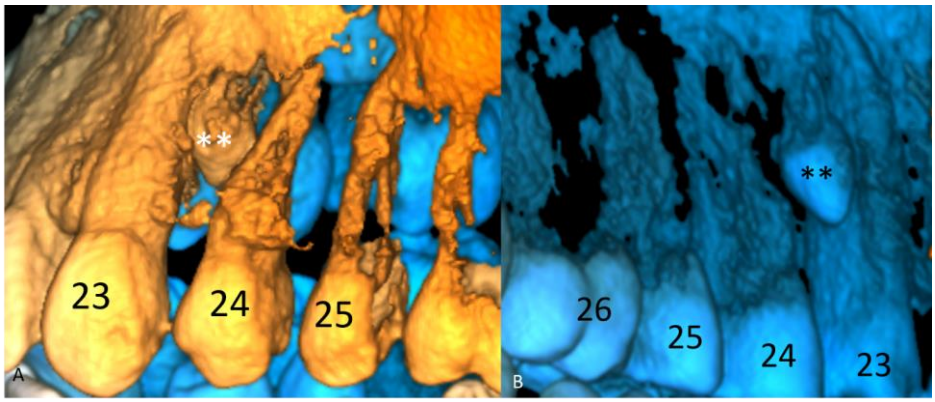

Fig. 79. Patient n°29. Planmeca 3D Mid CBCT. A. 3D lateral vestibular view of the left maxilla. Conical ST n°2 (**) close to the middle third of the adjacent root of the tooth n°24. B. 3D lateral vestibular posterior-anterior view of the left maxilla. Conical ST n°2 (**) slightly inclined to the vestibule.

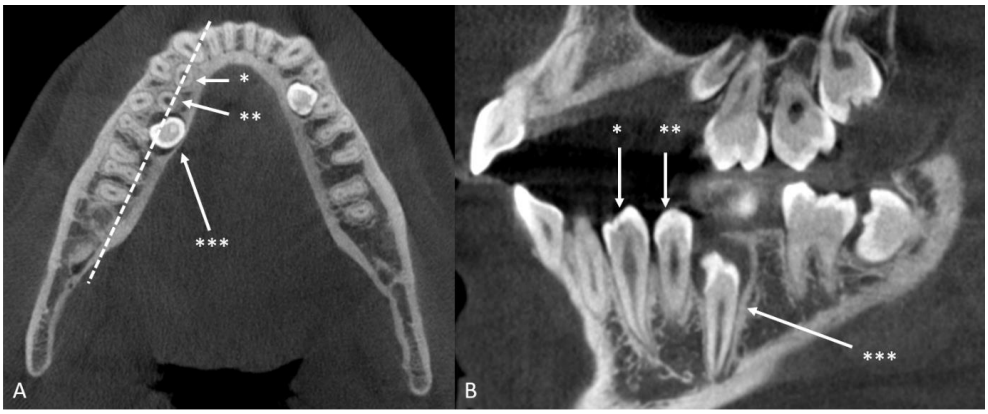

Fig. 80. Patient n°29. Planmeca 3D Mid CBCT. A. Axial view. ST n°3 (*) within the arch, and lingual to the root of the tooth n°44. ST n°4 (**) within the arch, and lingual to the root of the tooth n°45. ST n°5 (***) lingual to the mesial root of the tooth n°46. B. Parasagittal view through ST n°3, 4, 5 along the line with dashes from figure 80A. Supplemental, vertical, erupted ST n°3 (*). Supplemental, vertical, erupted ST n°4 (**). Supplemental, vertical, impacted ST n°5 (***).

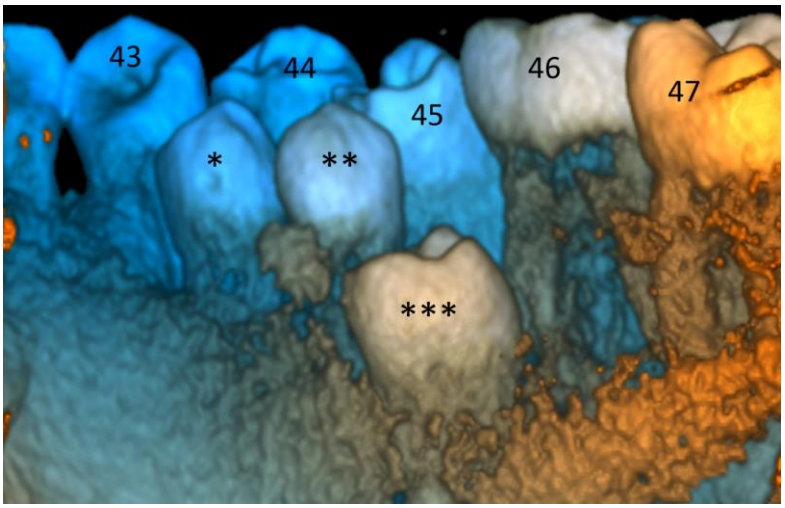

Fig. 81. Patient n°29. Planmeca 3D Mid CBCT. 3D lateral lingual view of the right mandible. Supplemental, vertical, erupted ST n°3 (*), lingual to the tooth n°44. Supplemental, vertical, erupted ST n°4 (**), lingual to the tooth n°45. Supplemental, vertical, impacted ST n°5 (***) with rotation with its mesial side oriented to the vestibule. ST n°5 (***) is lingual to the mesial root of the toot n°46.

Fig. 82. Patient n°29. Planmeca 3D Mid CBCT. A. Coronal view through ST n°3. ST n°3 (*) is of supplemental shape, vertical, erupted, and parallel to the tooth n°44. B. Coronal view through ST n°4. ST n°4 (**) is of supplemental shape, vertical, erupted, and parallel to the tooth n°45. Arrow: right foramen mentale. Close relationship between the apex of the ST n°4 (**) and the right inferior alveolar nerve canal. C. Coronal view through ST n°5. ST n°5 (***) is of supplemental shape, impacted, and slightly inclined to the lingual side. Close relationship between the apex of the ST n°5 (***) and the right inferior alveolar nerve canal (arrow).

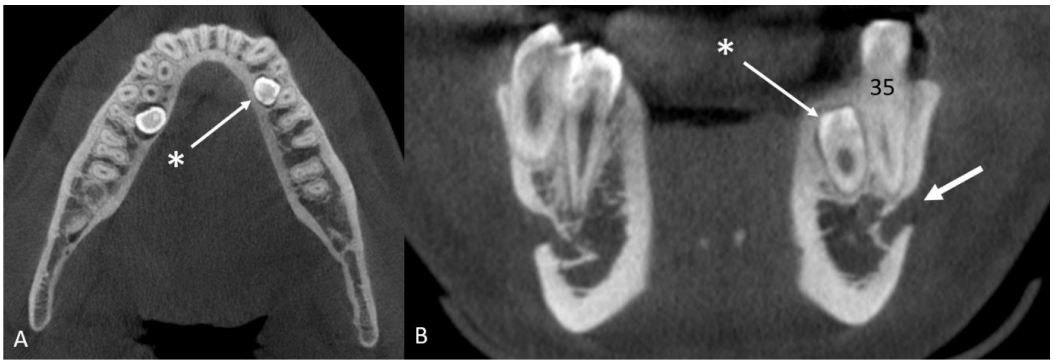

Fig. 83. Patient n°29. Planmeca 3D Mid CBCT. A. Axial view. ST n°6 (*) on the lingual side between the roots of the teeth n°34 and n°35. B. Coronal view. ST n°6 (*) of supplemental shape, lingual, impacted, and parallel to the tooth n°35. No relationship between the apex of the ST °6 (*) and the left foramen mentale (arrow).

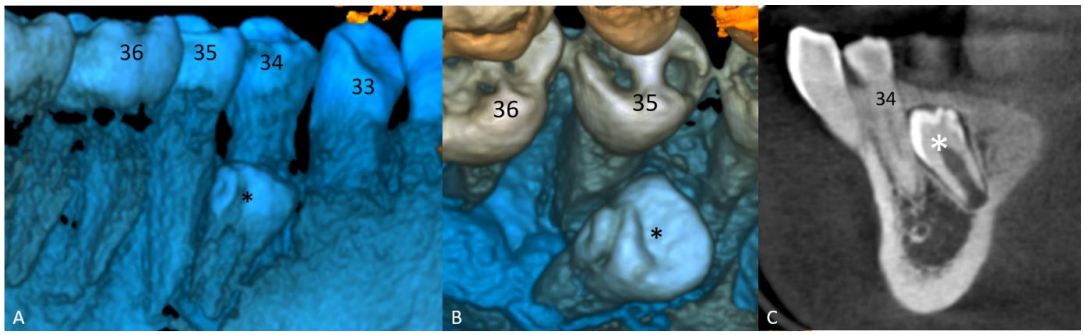

Fig. 84. Patient n°29. Planmeca 3D Mid CBCT. A. 3D lateral lingual view of the left mandible. ST n°6 (*) on the lingual side, close to the middle third of the root of the adjacent teeth n°34 and n°35. B. 3D occlusal view of the left mandible. ST n° 6 (*) in rotation, with its distal side oriented to the vestibule. C. Sagittal view. ST n°6 (*) inclined to the mesial side, and close to the middle third of the root of the adjacent teeth n°34, and without sign of external resorption.

Discussion

Mossaz et al provided until now with the most complete descriptive classification for ST in premolar and molar area [21]. Mossaz et al [21] and the majority of other authors [7-17] classified ST in relation with the crown location, the shape, the distribution, the position of ST in relation to normal adjacent teeth, and the state of ST eruption in relation with the adjacent teeth. The original contribution of Mossaz et al [21] was the addition of the description of the location of the cusp tip in relation with the closest erupted tooth, the follicle size measurement with less and more than 3mm. Mossaz et al provided also with a more precise description of the location of external root resorption by adjacent ST [21]. Some other authors added to the main ST classification the adjacent tooth complications due to the presence of ST, and types of damage to surrounding structures if removal of ST [10-12, 15, 25]. We developed our own classification matrix table for ST found in premolar and molar area (Table 1) which is based on previous classifications from the literature [7-13], and from the systematic article research from PubMed [1,2, 18-25].

1014 **Table 1. Classification of supernumerary teeth in premolar and molar**
1015 **area on CBCT.**

Location of the crown						
Axial view: transverse location	**Location on the arch**	**Location Anterior-posterior, in relation with adjacent tooth**				
	Labial/buccal [1, 15, 16, 21, 23, 24] (This study Fig. 34, 73-75)	Mesial/distal (This study Fig 18)				
	Within the arch/median [1, 16, 21, 24] (This study Fig. 22, 26, 27, 32, 35, 41, 44, 45, 46, 53, 58-60, 62-65, 67, 68, 78, 79)	Middle (This study Fig 1, 3, 5, 9, 12, 15-17, 29-31, 34-36, 37, 39, 40, 47, 48, 52, 69, 70, 78, 79)				
	Lingual/ palatine [1, 15, 16, 21, 23, 24] (Fig. 3, 5 of [21]) (This study Fig. 1, 3, 5, 9, 12, 15-18, 22 28, 30, 31, 37-40, 47-49, 52, 69, 70, 76, 77, 80-84)					
Coronal view: vertical location of the cusp tip in relation with closest erupted tooth [21]	Between the roots (This study Fig. 41-43)	Apical to the root tip [21] (This study Fig. 44-46, 53, 62-65)	Apical third of the root [21] (Fig. 5 of [21]) (This study Fig. 5, 8, 10, 13, 14, 16, 17, 19, 34-	Middle third of the root [21] (Fig. 4 of [2]), (Fig. 3 of [21]) (This study Fig 3, 22, 26, 27, 48, 52, 58-60, 76-79, 83, 84)	Cervical third of the root [21] (This study Fig. 28, 69-70)	Coronal [16, 21] (This study Fig. 1, 67, 68, 73-75, 80-82)

			37, 39, 40, 47-49, 53, 65)			
Shape: 3D reconstruction [10, 12, 21]	Supplemental (=eumorphic) [1, 10, 12, 14-17, 21, 23-25] (Fig. 4 of [2]), (Fig. 3 of [21]) (This study Fig. 1, 3, 5, 10, 22, 26-28, 64, 67, 68, 80-84)	Conical [1, 10, 12, 16, 17, 21-25] (This study Fig. 39-40, 44-46, 53, 58-60, 62, 63, 65, 69, 70, 76-79)	Tuberculate/ Molariform [1, 10, 12, 16, 17, 21-25] (This study Fig. 32, 36, 49-52)	Developing tooth bud [21] (Fig. 5 of [21]) (This study Fig. 12, 16-19, 21, 30, 31, 47-48, 65)	Under-sized (This study Fig. 34-43, 53)	Gemina-tion [22] (This study Fig. 73-75)
Distribution	Single [1, 10, 12, 14, 23] (Fig. 4 of [2]), (Fig. 2, 3, 5 of [21]) (This study Fig. 1, 3, 5, 10, 15-19, 21, 22, 26-28, 30-46, 64)	Multiple [1, 10, 12, 14] (This study Fig. 47-53, 58-60, 65, 67-70, 73-84)	Syndrome association [11, 12, 14, 23]	Unilateral [12, 23] (This study Fig. 1, 3, 5, 10, 15-19, 21, 22, 28, 30-46, 53, 62-64)	Bilateral [12] (This study Fig. 47-52, 58-60, 65, 67-70, 73, 75-80, 82-84)	
Position (in relation to normal tooth eruption): sagittal view [21]	Normal [1, 16, 21, 22, 24] (Fig. 3, 5 of [21]) (This study Fig. 1, 3, 5, 16-19, 26-28, 30, 31, 35-38, 44, 45, 47, 48, 50-53, 58, 59, 64, 65, 67-70, 73-75, 78-82)	Inclined [1, 16, 21, 22, 24] (Fig. 4 of [2]) (This study Fig. 10, 22, 26-28, 32, 34, 39-41, 43, 45, 50-52, 60, 65, 76, 77, 83, 84)	Transverse/ horizontal [1, 16, 21, 22, 24] (This study Fig. 46 62, 63)	Inverted [1, 15, 16, 21-24] (This study Fig. 32, 33)	Unde-finable [1, 21]	Fusion [18-20], (Fig. 2 of [18]), (Fig. 4, 5 of [19]), (Fig. 2 of [20]) (This study Fig. 73-75)
State of eruption of the supernumer-ary tooth: sagittal view [21]	Erupted [12, 15, 16, 21-24] (This study Fig. 1, 67, 68, 73-75, 80-82)	Impacted [12, 16, 21-24] (Fig. 4 of [2]) (Fig. 3, 5 of [21])				

		(This study Fig 3, 5, 10, 15-19, 21, 22, 26-28, 30-53, 58-60, 62-65, 69, 70, 73-79, 83 84)				
Follicle size measurement: sagittal view [21]	<3mm [21] (Fig. 3, 5 of [21]) (This study Fig. 5, 10, 12, 15-19, 22, 26, 30, 31, 39, 40, 44, 47, 49, 50, 52, 62, 63, 65, 73-79, 83,84)	>3 mm [21] (This study Fig. 46, 80, 82)	No follicle (This study Fig. 1, 3, 32, 34, 35 37, 41, 53, 57, 60, 67, 68, 80-82)	Dentigerous cyst [1, 11, 12, 15, 22-25] (This study Fig. 62-64)		
External root resorption of adjacent teeth by ST and its location in relation to the long axis of the involved tooth [1, 11, 21-25]	Cervical [21]	Middle [21]	Apical third of the root [21] (This study Fig. 50, 64)	The tip of the root [21] (This study Fig. 50)		
Internal resorption of ST	Crown (This study Fig. 64)	Root (This study Fig. 64)				
Adjacent tooth complication	Displacement [10-12, 16, 25] (This study Fig. 4, 14, 20, 32-34, 44, 45)	Rotation [1, 22, 25] (This study Fig. 5, 6)	Root dilaceration [25] (This study Fig. 14, 52)	Crowding [10-12, 23] (This study Fig. 73-75, 80-82)	Delayed/ failure of eruption [10-12, 15, 16, 22] (This study Fig. 2, 9, 32, 33, 44, 45, 58, 59, 67, 68)	Implant site prepara-tion [12]

Damage to surrounding structures if ST removal [11]	Inferior alveolar nerve [11] (This study Fig. 7, 8, 46, 82)	Foramen mentale [11] (Fig. 3B of [21] if extraction) (This study Fig. 20, 65)	Maxillary sinus [11] (This study Fig. 41, 76)	Damage to dental follicle/roots of permanent adjacent teeth [11, 15] (This study Fig. 58, 59)		

ST: supernumerary teeth

We added the description of the location of ST on axial view in anterior-posterior direction, the possibility of not existing follicle around ST, the location of the cusp or even of the complete ST between the roots of normally erupted teeth, a presence of undersized ST, and the presence/absence of internal resorption of ST. We don't add odontoma to our ST's classification as odontoma is classified as a benign tumor [28].

The ST classification on Table 1 contains 50 boxes. The 11 boxes were already illustrated by 8 figures freely available on Pubmed: 3 figures from Mossaz et al [21], 1 figure from Gurler et al [2], 1 figure from Zhu et al [18], 2 figures from Kato et al [19], and 1 figure from Cho et al [20]. 10 out of 11 boxes were illustrated only with 3 figures from Mossaz et al [21]. Our article freely provided with 84 figures. With our pictorial review we were able to illustrate 45 out of 50 boxes. We do not provide figures for syndromic patients as they were initially excluded from this review. The criterium of undefinable position of ST in relation to normal tooth eruption on sagittal view was insufficiently defined by Mossaz et al [21] to be illustrated. Root resorption of adjacent teeth by ST, and its cervical and middle location in relation to the long axis of the involved tooth [21] need still to be illustrated. Additionally, illustrations of ST on the site of the future dental implant are still missing [12].

The decision of naming ST or to give numbers to ST in case of hyperdontia and crowding of ST may be controversial, and it is open to discussion. We had problem to name ST in right mandibular premolar area of the patient n°28. We compared the size of the large impacted tooth with the size of the relatively smaller teeth present on the arch (Figure 68). We also compared Figure 68 with Figure 45 (transmigration and impaction of tooth n°44 because of ST which was positioned under the tooth n°84). We decided that the impacted premolar in the right mandible was the tooth n°44, and that two teeth on the arch above the impacted tooth were ST (44' and 44'') (Figure 68). We also decided that the tooth distal to the tooth called n°45 was a ST with the number n°45' (Figure 68), and that the tooth positioned lingually to the tooth n°35 (in occlusion with the upper arch) was a ST with the number n°35' (Figure 73). For the patient n°29 we decided to allocate numbers for additional teeth found on lingual side of the right mandible in premolar area (Figures 80, 81). Our

decision was met on the fact that buccaly positioned premolars were in occlusion with the upper arch, and that labial/buccal location seems to be rarer than lingual/palatine position for the presence of ST (Figures 80, 81).

We provided only two examples of performed panoramic X-rays before CBCT (Figures 65A, and 66) to show the limitation of this technique in finding existing ST, in classifying ST, and in indicating the risk of complications related to the presence of ST [1, 2]. On the other hand, 2D reformatted views and 3D CBCT reconstruction were useful to understand the 3D position of ST in relation with adjacent teeth (Figure 43), to describe ST involved in troubles of eruption of normal teeth, in delayed teeth permutation (Figures 45, 58), and to understand complex ST topography with crowding of multiple types of ST (figures 56, 58, 68, 73, 81). We also used 3D CBCT reconstruction along with modification of the threshold in patients with motion artifacts where 2D images were more difficult to interpret (Figures 28-29, 47-48) [27].

Finally, our pictorial review was able to freely provide the readership with more complete description of ST in premolar and molar area on CBCT than in already published studies.

- **Acknowledgements**: none
- **Funding sources statement**: This study does not receive any funding.
- **Competing interests**: Prof R. Olszewski is the Editor-in-Chief of NEMESIS. The other authors declare no conflict of interest.
- **Ethical approval**: We obtained the approval from our University and Hospital Ethical committee for this study (B403/2019/03DEC/542).
- **Informed consent**: Patients n°1-12, n°14-22, n°24, n°25, and n°29 were exempted from the informed consent according to the ethical committee approval. We obtained a written informed consent from the patient n°28. There was no need for informed consent for patients n°13, n°23, n°26, n°27 as all the images were anonymized, and no private data were provided allowing the patient's identification.

Authors contribution:

Author	Contributor role
Olszewski Raphael	Conceptualization, Investigation, Methodology, Data curation, Resources, Validation, Writing original draft preparation, Supervision, Writing review and editing
Shimwa-Karengera Stéphane	Investigation, Methodology, Validation, Writing original draft preparation, Writing review and editing
Gurniak Anna	Data curation, Validation, Writing review and editing
Gurniak Eliza	Data curation, Validation, Writing review and editing
Simain Sato Franklin	Data curation, Validation, Writing review and editing

References

1. Ma Ma X, Jiang Y, Ge H, Yao Y, Wang Y, Mei Y, Wang D. Epidemiological, clinical, radiographic characterization of non-syndromic supernumerary teeth in Chinese children and adolescents. Oral Dis 2021;27:981-992. doi: 10.1111/odi.13628.

2. Gurler G, Delilbasi C, Delilbasi E. Investigation of impacted supernumerary teeth: a cone beam computed tomograph (cbct) study. J Istanb Univ Fac Dent 2017;51:18-24. doi: 10.17096/jiufd.20098.

3. Olszewski R, Theys S, Perez E, Wisniewska K, Wisniewski M. Revue illustrée des principales indications de CBCT en orthodontie. Nemesis 2020;12:1-15. https://doi.org/10.14428/nemesis.v12i1.

4. Kapila S, Conley RS, Harrell WE Jr. The current status of cone beam computed tomography imaging in orthodontics. Dentomaxillofac Radiol 2011;40:24-34. doi: 10.1259/dmfr/12615645.

5. Kapila SD, Nervina JM. CBCT in orthodontics: assessment of treatment outcomes and indications for its use. Dentomaxillofac Radiol 2015;44:20140282. doi: 10.1259/dmfr.20140282.

6. Deepti A, Muthu MS. Supernumerary teeth: review of literature and decision support system. Indian J Dent Res 2013;24:117-122. doi: 10.4103/0970-9290.114911.

7. Di Biase DD. Midline supernumeraries and eruption of the maxillary central incisor. Dent Pract Dent Rec 1969;20:35-40.

8. Foster TD, Taylor GS. Characteristics of supernumerery teeth in the upper central incisor region. Dent Pract Dent Rec 1969;20:8-12.

9. Primosch RE. Anterior supernumerary teeth--assessment and surgical intervention in children. Pediatr Dent 1981;3:204-215.

10. Mitchell L. Supernumerary teeth. Dent Update 1989;16:65-66, 68-69.

11. Scanlan PJ, Hodges SJ. Supernumerary premolar teeth in siblings. Br J Orthod 1997;24:297-300. doi: 10.1093/ortho/24.4.297.

12. Garvey MT, Barry HJ, Blake M. Supernumerary teeth--an overview of classification, diagnosis and management. J Can Dent Assoc 1999;65:612-616.

13. Patchett CL, Crawford PJ, Cameron AC, Stephens CD. The management of supernumerary teeth in childhood-a retrospective study of practice in Bristol Dental Hospital, England and Westmead Dental Hospital, Sydney, Australia. Int J Paediatr Dent 2001;11:259-265. doi: 10.1046/j.1365-263x.2001.00282.x.

14. Kalra N, Chaudhary S, Sanghi S. Non-syndrome multiple supplemental supernumerary teeth. J Indian Soc Pedod Prev Dent 2005;23:46-48. doi: 10.4103/0970-4388.16029.

15. Fernández-Montenegro P, Valmaseda-Castellón E, Berini-Aytés L, Gay-Escoda C. Retrospective study of 145 supernumerary teeth. Med Oral Patol Oral Cir Bucal 2006;11:339-344.

16. De Oliveira Gomes C, Neves Drummond S, Correia Jham B, Neves Abdo E, Alves Mesquita R. A survey of 460 supernumerary teeth in Brazilian children and adolescents. Int J Paediatr Dent 2008;18:98-106. doi: 10.1111/j.1365-263X.2007.00862.x.

17. Ferrés-Padró E, Prats-Armengol J, Ferrés-Amat E. A descriptive study of 113 unerupted supernumerary teeth in 79 pediatric patients in Barcelona. Med Oral Patol Oral Cir Bucal 2009;14:146-152.

18. Zhu M, Liu C, Ren S, Lin Z, Miao L, Sun W. Fusion of a supernumerary tooth to right mandibular second molar: a case report and literature review. Int J Clin Exp Med 2015;8:11890-11895 ;

19. Kato H, Kamio T. Diagnosis and endodontic management of fused mandibular second molar and paramolar with concrescent supernumerary tooth using cone-beam CT and 3-D printing technology: a case report. Bull Tokyo Dent Coll 2015;56:177-184. doi: 10.2209/tdcpublication.56.177

20. Cho KM, Jang JH, Park SH. Clinical management of a fused upper premolar with supernumerary tooth: a case report. Restor Dent Endod 2014;39:319-323. doi: 10.5395/rde.2014.39.4.319.].

21. Mossaz J, Kloukos D, Pandis N, Suter VG, Katsaros C, Bornstein MM. Morphologic characteristics, location, and associated complications of maxillary and mandibular supernumerary teeth as evaluated using cone beam computed tomography. Eur J Orthod 2014;36:708-718. doi: 10.1093/ejo/cjt101.

22. Liu DG, Zhang WL, Zhang ZY, Wu YT, Ma XC. Three-dimensional evaluations of supernumerary teeth using cone-beam computed tomography for 487 cases. Oral

Surg Oral Med Oral Pathol Oral Radiol Endod 2007;103:403-411. doi: 10.1016/j.tripleo.2006.03.026.

23. Chen KC, Huang JS, Chen MY, Cheng KH, Wong TY, Huang TT. Unusual supernumerary teeth and treatment outcomes analyzed for developing improved diagnosis and management plans. J Oral Maxillofac Surg 2019;77:920-931. doi: 10.1016/j.joms.2018.12.014.

24. Jiang Y, Ma X, Wu Y, Li J, Li Z, Wang Y, Cheng J, Wang D. Epidemiological, clinical, and 3-dimentional CBCT radiographic characterizations of supernumerary teeth in a non-syndromic adult population: a single-institutional study from 60,104 Chinese subjects. Clin Oral Investig 2020;24:4271-4281. doi: 10.1007/s00784-020-03288-3.

25. Merrett SJ, Drage N, Siphahi SD. The use of cone beam computed tomography in planning supernumerary cases. J Orthod 2013;40:38-46. doi: 10.1179/1465313312Y.0000000029.

26. Dive B, Aps JKM, Huljev D, Gurniak A, Klein-DębekE , Beyls H, Hebda A, Olszewski R. Cone beam computed tomography in the diagnosis of Stafne bone cavity: Report of seven cases and review of the open-access literature. Nemesis 2021;18:1-20. https://doi.org/10.14428/nemesis.v18i1

27. Olszewski R. Open access resources on motion artifact in adult dentomaxillofacial CBCT: illustrated pictorial review of medical literature. Nemesis 2021;15:1-37. https://doi.org/10.14428/nemesis.v15i1

28. Koenig LJ. Diagnostic Imaging: Oral and Maxillofacial. Amirsys Ed, 2012, Salt Lake City, United States, 1000 pages, ISBN10 193188420X